

1 We thank the Associate Editor and two referees for their providing constructive comments to this  
2 manuscript. Below we detail how we have revised the manuscript following their suggestions.

3 1. The problem of more degrees of freedom with more details models is equifinality: several  
4 combinations of parameters match the data similarly well. That needs to be incorporated in  
5 forward simulations, which usually become more uncertain with equifinality.

6 *Response: Thanks for the comments. To address the impacts of “equifinality” on our*  
7 *quantifications associated with parameters, we have conducted ensemble simulations for both*  
8 *20<sup>th</sup> and 21<sup>st</sup> centuries with respect to uncertain parameters. These ensemble simulations shall*  
9 *cover the “equifinality” set of parameters in our model. In other words, these simulations shall*  
10 *have included the “equifinality” impacts. We presented the simulations results in Figure 11 and*  
11 *Figure 12 in this revision.*

12 2. Fig 3: It is not clearly stated, how many parameters were calibrated and Fig. 3 is barely  
13 readable because of display quality. Are there only 3 out of the 6 sites displayed?

14 *Response: Thanks for the comments. We have revised Figure 3. Now six sites are shown and the*  
15 *figure shall be more readable.*

16 3. Cost function (17): Why did you not consider uncertainty of observed NEE? Usually, you  
17 need this to determine, which parameter sets are viable. If you have larger NEE confidence  
18 bounds, also more different parameter sets will generate predictions that are still compatible with  
19 the calibration NEE. For my main concern above it is important to keep also the slightly less  
20 optimal but compatible parameter sets.

21 *Response: The error or uncertainty of the NEE data we used have not been provided by field*  
22 *experimentalists. Thus, in this study, the model parameters are only constrained by the observed*  
23 *magnitudes and temporal variabilities of NEE at those sites.*

24

25

26

1 **Microbial dormancy and its impacts on Arctic terrestrial ecosystem carbon budget**

2

3 Junrong Zha and Qianlai Zhuang

4

5 Department of Earth, Atmospheric, and Planetary Sciences and Department of Agronomy,  
6 Purdue University, West Lafayette, IN 47907 USA

7

8 Submitted to: *Biogeoscience*

9

10 Correspondence to: qzhuang@purdue.edu

11

12

13

14

15

16

17

18

19

20

21

22

23

24

25

26

27

28

29

30

31

32

33

34

35

36

37

38

39

40

41

42

43

44

45

46

47 **Abstract**

48 **A large amount of soil carbon in the Arctic terrestrial ecosystems could be emitted as**  
49 **greenhouse gases in a warming future. However, lacking detailed microbial processes such**  
50 **as microbial dormancy in current biogeochemistry models might have biased the**  
51 **quantification of the regional carbon dynamics. Here the effect of microbial dormancy was**  
52 **incorporated into a biogeochemistry model to improve the quantification for the last and**  
53 **this century. Compared with the previous model without considering the microbial**  
54 **dormancy, the new model estimated the regional soils stored 75.9 Pg more C in the**  
55 **terrestrial ecosystems during the last century, and will store 50.4 Pg and 125.2 Pg more C**  
56 **under the RCP 8.5 and RCP 2.6 scenarios, respectively, in this century. This study**  
57 **highlights the importance of the representation of microbial dormancy in earth system**  
58 **models to adequately quantify the carbon dynamics in the Arctic.**

59

60

61

62

63

64

65

66

67

68

69

70

71

72

73

74

75

## 76 1. Introduction

77 The land ecosystems in northern high latitudes ( $>45^{\circ}\text{N}$ ) occupy 22% of the global  
78 surface and store over 40% of the global soil organic carbon (SOC) (McGuire & Hobbie, 1997;  
79 Melillo et al., 1993; Tarnocai et al., 2009; Hugelius et al., 2014). During the past decades, a  
80 greening accompanying a warming in the region has been documented (Zhou et al., 2001; Lloyd  
81 et al., 2002; Stow et al., 2004; Callaghan et al., 2005; Tape et al., 2006). The regional carbon  
82 dynamics are expected to loom large in the global carbon cycle and exert large feedbacks to the  
83 global climate system (McGuire et al., 2009; Davidson & Janssens, 2006; Bond-Lamberty &  
84 Thomson, 2010).

85 To date, numerous ecosystem models have been developed to project the feedbacks  
86 between terrestrial ecosystem carbon cycling and climate (Raich et al., 1991; Zhuang et al.,  
87 2001, 2002, 2015; Parton et al., 1993; Knorr et al., 2005; Running & Coughlan, 1988), but they  
88 can bias their quantifications due to missing detailed microbial mechanisms in these models  
89 (Schmidt et al., 2011; Todd-Brown et al., 2013; Conant et al., 2011; Treseder et al., 2011).  
90 Microorganisms play a central role in decomposition of litter and soil organic carbon, which  
91 further governs the global carbon cycling and climate change (Xu et al., 2014; Treseder et al.,  
92 2011; Wang et al., 2015). An emerging field of research has begun to incorporate microbial  
93 ecology into existing process-based models ~~to remedy the to represent decomposition in ways~~  
94 ~~that include important microbial processes that were previously ignored~~ inadequate representation  
95 of soil decomposition process (Zha & Zhuang, 2018; Schimel & Weintraub, 2003; Allison et al.,  
96 2010; German et al., 2012). These microbial-based models tend to better reproduce field and  
97 satellite observations than traditional ones that treat soil decomposition as a first-order decay  
98 process without considering microbial activities (Treseder et al., 2011; Wieder et al., 2013;

99 Todd-Brown et al., 2011; Lawrence et al., 2009; Moorhead et al., 2006). However, some vital  
100 microbial traits such as microbial dormancy and community shifts are still rarely explicitly  
101 considered in large-scale ecosystem models ([Wieder et al., 2015](#)), and this may introduce notable  
102 uncertainties (Graham et al., 2014, 2016; Wang et al., 2015; Bouskill et al., 2012; Kaiser et al.,  
103 2014).

104 Dormancy is broadly recognized as a strategy for microorganisms to cope with periodical  
105 environmental stresses (Harder & Dijkhuizen, 1983). When environmental conditions are  
106 unfavorable for growth, microbes switch to a dormant state, which is a reversible state of low to  
107 zero metabolic activity (Stolpovsky et al., 2011; Lennon & Jones, 2011). In this state,  
108 biogeochemical processes such as soil decomposition are slow (Blagodatskaya et al., 2013). At  
109 any given time, there is only a fraction of ~~-, likely below 50%, -of metabolically active microbes in~~  
110 ~~natural soils~~ [number of microbes, likely below 50% of live microbes,](#) in natural soils (Wang et  
111 al., 2015; Stolpovsky et al., 2011). Soil decomposition and nutrient cycling mainly depend on  
112 these active microbes because only active ones can consume organic matter and replicate  
113 themselves (Wang et al., 2015; Blagodatskaya et al., 2014). To date, most existing  
114 biogeochemistry models [use total rather than active microbial biomass as an indicator of](#)  
115 [microbial activities \(Wieder et al., 2015\)](#) ~~used total microbial biomass as indicator of microbial~~  
116 ~~activities, rather than the active portion of microbial biomass,~~ which could bias the estimates of  
117 soil decomposition and ecosystem carbon budget (Hagerty et al., 2014; He et al., 2015).  
118 Especially, the Arctic terrestrial ecosystems are nitrogen-limited, neglecting microbial dormancy  
119 will lead to incorrect estimates of nitrogen availability through soil decomposition, failing to  
120 capture nitrogen feedbacks to carbon dynamics (Wang et al., 2015; Stolpovsky et al., 2011;  
121 Thullner et al., 2005). [Furthermore, the Arctic](#) ~~Besides, it is also important because of~~ [has](#)

122 ~~experienced a the marked seasonality of (i.e. active and dormant microbial cycles) and the~~  
123 ~~above-global-average warming, happening in those latitudes (which might could have increased~~  
124 ~~the proportion of active microbes in soils) (He et al., 2015).~~ Thus, incorporating dormancy  
125 effects will improve model realism ~~to and show the important role of microbial dormancy~~  
126 ~~provide a better in provide a better the~~ projection of the Arctic carbon dynamics.

127 This study incorporated the effects of microbial dormancy trait into an extant process-  
128 based biogeochemistry model (MIC-TEM) (Zha & Zhuang, 2018; He et al., 2015). The dormant  
129 and active microbial physiology has been considered explicitly in the new version of model  
130 (MIC-TEM-dormancy). The revised model was parameterized, validated, and then applied to  
131 evaluate the carbon dynamics during the last and this centuries in the Arctic terrestrial  
132 ecosystems (north 45 °N above). ~~By comparing the results of MIC-TEM-dormancy and MIC-~~  
133 ~~TEM, we can show that incorporating microbial dormancy may produce a much different~~  
134 ~~prediction in historical and future carbon budget.~~  
135 ~~and demonstrate the essential role of microbial dormancy.~~

## 137 2. Methods

### 138 2.1 Overview

139 ~~Due to the importance of microbial dormancy, some recent work has been done to consider~~  
140 ~~the metabolic activation and deactivation of microbes in soil and its effects on soil carbon (C)~~  
141 ~~dynamics and climate feedbacks (Wang et al., 2015; Salazar et al., 2018).~~ For example, Wang et  
142 ~~al. (2015) has incorporated transformation processes between active and dormant states to~~  
143 ~~developed two versions of MEND, that is, MEND with and without dormancy. The two versions~~  
144 ~~of the model have been applied to quantify model the carbon decomposition in of laboratory~~

145 incubations of four soils. Salazar et al. (2018) have also taken ~~ook~~ microbial dormancy into  
146 account to compare their predictions of microbial biomass and soil heterotrophic respiration (R<sub>H</sub>)  
147 under simulated cycles of stressful (dryness) and favorable (wet pulses) conditions. Our study  
148 extend those modeling studies to the whole Arctic region by developing a more detailed  
149 biogeochemistry model considering the dormancy impacts. In ~~Below, this paper, first,~~ we first  
150 describe how we developed ~~d~~ the new model (MIC-TEM-dormancy) by incorporating the  
151 microbial dormancy trait into an existing microbial-based biogeochemistry model (MIC-TEM).  
152 Second, we discuss how ~~conduct the~~ parameterization and validation of MIC-TEM-dormancy  
153 model were conducted using observed net ecosystem exchange data, and heterotrophic respiration  
154 data at representative sites ~~have been shown~~. Third, we presented how ~~applied~~ the model was  
155 applied to ~~to~~ northern high latitudes (above 45 °N) for the 20<sup>th</sup> and 21<sup>st</sup> centuries and ~~discussed~~  
156 to demonstrate the dormancy effects on regional carbon budget.

157

## 158 **2.2 Model description.**

159 A non-dormancy version of biogeochemistry model (MIC-TEM) has been developed by  
160 incorporating a microbial module (Allison et al., 2010) into an extant large-scale biogeochemical  
161 model (TEM) to explicitly (Zhuang et al., ~~2001, 2002,~~ 2003) consider the effects of microbial  
162 dynamics and enzyme kinetics on carbon dynamics (Zha & Zhuang, 2018). Here we further  
163 advanced the MIC-TEM by incorporating algorithms that describe the effects of microbial  
164 dormancy dynamics based on He et al. (2015). Different from He et al. (2015), in which  
165 microbial module was driven with existing data of carbon stocks and fluxes, our study  
166 incorporated the microbial module into an extant MIC-TEM that simulates carbon data  
167 dynamically. This coupling enables us to extrapolate our model to whole northern high-latitudes

168 region, rather than only for temperate forest region in He et al. (2015). In our new model (MIC-  
169 TEM-dormancy), microbial biomass pool was divided into two fractions, including the dormant  
170 and active microbial biomass pools. The two microbial biomass pools and the reversible  
171 transition between them have been considered explicitly in the new model (Figure 1), which was  
172 ignored in MIC-TEM (Figure 1).

173 In previous MIC-TEM, heterotrophic respiration ( $R_H$ ) is calculated as:

$$174 \quad R_H = \text{ASSIM} * (1 - \text{CUE}) \quad (1)$$

175 Where ASSIM and CUE represent microbial assimilation and carbon use efficiency, respectively.

176 For detailed carbon dynamics in MIC-TEM, see Zha & Zhuang (2018).

177 Here we revised MIC-TEM by incorporating microbial dormancy dynamics according to  
178 He et al. (2015). In the new model (MIC-TEM-dormancy), the soil heterotrophic respiration  $R_H$  is  
179 comprised of three parts: the maintenance respiration from the active and dormant microorganisms  
180 and the  $\text{CO}_2$  production through the process of microbial assimilation (He et al., 2015):

$$181 \quad R_H = m_R Q_{10\text{mic}}^{\frac{\text{temp}-15}{10}} B_a + \beta m_R Q_{10\text{mic}}^{\frac{\text{temp}-15}{10}} B_d + \text{CO}_2 \quad (2)$$

182 where the first two terms are maintenance respiration from the active and dormant  
183 microorganisms, respectively. The last term is the  $\text{CO}_2$  produced during the process of microbial  
184 assimilation.

185 For first two terms,  $B_a$  and  $B_d$  represents the active and dormant microbial biomass pool,  
186 respectively. The parameter  $m_R$  denotes the specific maintenance rate at active state ( $\text{h}^{-1}$ ), and  $\beta$   
187 is the ratio of dormant maintenance rate to active maintenance rate. Thus,  $\beta m_R$  denotes the  
188 maximum specific maintenance rate at dormant state. Temperature sensitivity was expressed as

189 the  $Q_{10}$  function ( $Q_{10}^{\frac{\text{temp}-15}{10}}$ ), where temp is soil temperature at top 20 cm (units:  $^{\circ}\text{C}$ ).



190 For the third term, the CO<sub>2</sub> produced through microbial assimilation is calculated as in He et al.  
 191 (2015) and Allison et al. (2010):

$$192 \quad \text{CO}_2 = \text{ASSIM} * (1 - Y_g) \quad (3)$$

193 Where ASSIM represents the ~~variable of~~ microbial assimilation and the parameter Y<sub>g</sub> represents  
 194 carbon use efficiency. Microbial assimilation (ASSIM) is calculated as in He et al. (2015):

$$195 \quad \text{ASSIM} = \frac{1}{Y_g} \frac{\Phi}{\alpha} m_R Q_{10enz}^{\frac{\text{temp}-15}{10}} \text{Ba} \left( \frac{\text{CN}_{\text{soil}}}{\text{CN}_{\text{mic}}} \right)^{0.6} \quad (4)$$

196 Here parameter α is ~~called the~~ maintenance weight (h<sup>-1</sup>), CN<sub>soil</sub> and CN<sub>mic</sub> denotes the C:N ratios  
 197 of soil and that of microbial biomass ~~to consider substrate quality~~. Besides, Φ is ~~the called~~ substrate  
 198 saturation level and defined as in He et al. (2015) and Wang et al. (2014):

$$199 \quad \Phi = \frac{S}{K_s + S} \quad (5)$$

200 Where K<sub>s</sub> is the half saturation constant for substrate uptake as indicated by the Michaelis–Menten  
 201 kinetic, and S is soluble C substrates that are directly accessible for microbial assimilation (Wang  
 202 et al., 2014). Here we quantified concentration of soluble C substrates that are directly accessible  
 203 for microbial assimilation by using conceptual framework from Davidson et al. (2012):

$$204 \quad S = \text{Soluble C} * D_{\text{liq}} * \theta^3 \quad (6)$$

205 The term ‘Soluble C’ denotes the state variable of soluble carbon pool. D<sub>liq</sub> is the diffusion  
 206 coefficient of the substrate in the liquid phase, and is formulated as:

$$207 \quad D_{\text{liq}} = 1 / (1 - \text{BD} / \text{PD})^3 \quad (7):$$

208 Where BD is the bulk density and PD is the soil particle density. θ is the volumetric soil moisture.

209 Different from MIC-TEM, the transitions between active and dormant microbial biomass are  
 210 included in MIC-TEM-dormancy. ~~We used B<sub>a→d</sub> and B<sub>d→a</sub> denotes the transition from the active~~

211 ~~to dormant microbe and from the dormant to active microbe, respectively (He et al., 2015; Wang~~  
 212 ~~et al., 2014):~~

$$213 \quad B_{a \rightarrow d} = (1 - \Phi) m_R Q_{10mic}^{\frac{temp-15}{10}} B_a \quad (87)$$

$$214 \quad B_{d \rightarrow a} = \Phi m_R Q_{10mic}^{\frac{temp-15}{10}} B_d \quad (98)$$

215 Where  $B_{a \rightarrow d}$  and  $B_{d \rightarrow a}$  denote the transition from the active to dormant microbe and from the  
 216 dormant to active microbe, respectively (He et al., 2015; Wang et al., 2014).

217 Thus, dDormancy rate is affected by active and dormant biomass, substrate availability ( $B_a, B_d$ ),  
 218 soil temperature (temp) and soil moisture ( $\theta$  in  $\Phi$ ).

219 The active microbial biomass ( $B_a$ ) is modeled as (He et al., 2015; Wang et al., 2014):

$$220 \quad \frac{dB_a}{dt} = ASSIM * Y_g - m_R Q_{10mic}^{\frac{temp-15}{10}} B_a - B_{a \rightarrow d} + B_{d \rightarrow a} - DEATH - EPROD \quad (109)$$

221 Where DEATH and EPROD denotes microbial biomass death and enzyme production, which are  
 222 modeled as proportional to active microbial biomass with constant rates  $r_{death}$  and  $r_{EnzProd}$  (Allison  
 223 et al., 2010):

$$224 \quad DEATH = r_{death} * B_a \quad (110)$$

$$225 \quad EPROD = r_{EnzProd} * B_a \quad (124)$$

226 Where  $r_{death}$  and  $r_{EnzProd}$  are the rate constants of microbial death and enzyme production,  
 227 respectively.

228 The dormant microbial biomass ( $B_d$ ) is modeled as (He et al., 2015; Wang et al., 2014):

$$229 \quad \frac{dB_d}{dt} = -\beta m_R Q_{10mic}^{\frac{temp-15}{10}} B_d + B_{a \rightarrow d} - B_{d \rightarrow a} \quad (132)$$

230 The Soluble C pool is modeled as (He et al., 2015; Allison et al., 2010):

$$231 \quad \frac{d \text{Soluble C}}{dt} = DECAy - ASSIM + ELOSS + DEATH \quad (143)$$

232 Where DECAF represents the enzymatic decay of soil organic carbon (SOC), and ELOSS  
233 represents the loss of enzyme.

234 DECAF is regulated by enzyme biomass (ENZ), soil organic carbon (SOC), soil temperature, and  
235 substrate quality (He et al., 2015):

$$236 \quad \text{DECAF} = V_{\text{max}} * Q_{10\text{enz}}^{\frac{\text{temp}-15}{10}} * \text{ENZ} * \frac{\text{SOC}}{K_{\text{muptake}} + \text{SOC}} * (120 - \text{CN}_{\text{soil}}) \quad (154)$$

237 Where  $V_{\text{max}}$  is the maximum SOC decay rate,  $K_{\text{muptake}}$  is half saturation constant for enzymatic  
238 decay.

239 ELOSS is modeled as a first-order process (Allison et al., 2010) to represent enzyme turnover:

$$240 \quad \text{ELOSS} = r_{\text{enzloss}} * \text{ENZ} \quad (165)$$

241 Where  $r_{\text{enzloss}}$  is the rate constant of enzyme loss.

242 The soil organic carbon pool (SOC) is modeled as:

$$243 \quad \frac{d\text{SOC}}{dt} = \text{Litterfall} - \text{DECAF} \quad (176)$$

244 Where Litterfall is estimated as a function of vegetation carbon (Zhuang et al., 2010).

245 Last, enzyme pool (ENZ) is modeled as:

$$246 \quad \frac{d\text{ENZ}}{dt} = \text{EPROD} - \text{ELOSS} \quad (187)$$

247 With the modification of microbial carbon dynamics by considering microbial life-history trait,  
248 soil decomposition is changed since it is controlled by microbes. When microbial dormancy is  
249 considered, the number of active microbes that participate in soil decomposition is much less than  
250 that we considered before different. The changes in soil decomposition directly influence the  
251 amount of soil respiration, and further influence soil nitrogen (N) mineralization that determines  
252 soil N availability for plants, affecting gross primary production (GPP). Since both GPP and soil

253 ~~respiration~~ ( $R_H$ ) can be affected by microbial dormancy, net ecosystem production (NEP) will also  
254 be affected.

255

### 256 **2.3 Model parameterization and validation**

257 The detailed description of parameters that are related to microbial dormancy can be found  
258 in He et al. (2015) (Table 1). Here we calibrated the MIC-TEM-dormancy at six representative  
259 sites with gap-filled monthly net ecosystem productivity (NEP,  $\text{gCm}^{-2}\text{mon}^{-1}$ ) data in northern high  
260 latitudes (Table 2). Site-level climatic data and soil texture data were organized for driving model.  
261 All sites information can be found on AmeriFlux network (Davidson et al., 2000). The results for  
262 model parameterization were presented in Figure 2. We conducted the parameterization using a  
263 global optimization algorithm known as SCE-UA (Shuffled complex evolution) method (Duan et  
264 al., 1994). An ensemble of 50 independent sets of parameters were performed based on prior ranges  
265 from literature (Table 1) to minimize the difference between the monthly simulated and measured  
266 NEP at the chosen sites. The cost function of the minimization is:

$$267 \quad \text{Obj} = \sum_{i=1}^k (\text{NEP}_{\text{obs},i} - \text{NEP}_{\text{sim},i})^2 \quad (17)$$

268 Where  $\text{NEP}_{\text{obs},i}$  and  $\text{NEP}_{\text{sim},i}$  are the observed and simulated NEP, respectively.  $k$  is the number of  
269 data pairs for comparison. Except for the parameters of microbial dormancy, other parameters are  
270 derived directly from MIC-TEM (Zha & Zhuang, 2018). The optimized parameters were used for  
271 model validation and regional simulations.

272 For model validation, we chose another six sites that containing monthly NEP data from  
273 AmeriFlux network (Table 3). Moreover, we also conducted site-level validations with monthly  
274 soil respiration data from AmeriFlux network and Fluxnet dataset. The site information was  
275 provided in Table 4. For these sites, we assumed 50% of soil respiration was heterotrophic

276 respiration ( $R_H$ ) for forest (Hanson et al., 2000), 60% and 70% of that was  $R_H$  for grassland (Wang  
277 et al., 2009) and tundra (Billings et al., 1977). Because there is a -of-limited ations in the amount  
278 of available  $R_H$  data~~there is a limited amount of measured data of heterotrophic respiration~~, we  
279 could not conduct a regional validation for all pixels in northern high latitudes. Instead, we  
280 extracted 61 sites providing data of average annual heterotrophic respiration from ORNL global  
281 Soil Respiration Dataset ([https://daac.ornl.gov/SOILS/guides/SRDB\\_V4.html](https://daac.ornl.gov/SOILS/guides/SRDB_V4.html), Bond-Lamberty et  
282 al., 2018) for model validation. The site-level observed average annual  $R_H$  was used to compare  
283 with simulated annual  $R_H$  by MIC-TEM-dormancy and MIC-TEM. The ~~new model~~(MIC-TEM-  
284 dormancy) was run at monthly time step to keep consistent with the time step of MIC-TEM.  
285 Although microbial dynamics occur at fine temporal scales (Tang & Riley, 2014), we can still  
286 quantify the cumulative impacts of microbial dynamics on carbon and nitrogen cycling at monthly  
287 time by not changing the model structure.

288

## 289 2.4 Spatial extrapolation

290 For historical simulations during the 20<sup>th</sup> century, two sets of regional simulations using  
291 MIC-TEM-dormancy and MIC-TEM at a spatial resolution of  $0.5^\circ$  latitude  $\times$   $0.5^\circ$  longitude were  
292 conducted. Our model simulation contains two parts: spin-up and transient simulation. A typical  
293 spin-up was conducted to get the model to a steady state for each spatial location, which will be  
294 used as initial conditions for transient simulations (McGuire et al., 1992). During spin-up  
295 procedure, cyclic forcing data was used to force the model run, and repeated continuously until  
296 dynamic equilibrium was achieved at which the modeled state variables show a cyclic pattern or  
297 become constant. Specifically, this study used the monthly historical climate data from 1900 to  
298 1940 to repeatedly drive the model for the spin-up. Before spin-up procedure, the model was

299 initialized with default built-in carbon stocks (Raich et al., 1991). During transient simulations,  
300 the calibrated ecosystem-specific parameters were used for regional simulations. The previous  
301 dynamic equilibrium was used as initial value for transient simulation. The historical climatic  
302 forcing data, including the monthly air temperature, precipitation, cloudiness, and atmospheric  
303 CO<sub>2</sub> concentrations, were organized from the Climatic Research Unit (CRU TS3.1) from the  
304 University of East Anglia (Harris et al., 2014). We also used gGridded data of soil texture (Zhuang  
305 et al., 2003), elevation (Zhuang et al., 2015), and potential natural vegetation (Melillo et al., 1993)  
306 from literatures ~~were also used~~. In our model, we assumed that soil texture, elevation, and potential  
307 natural vegetation data only vary spatially, not vary over time (Zhuang et al., 2015).

308 In addition, regional simulations over the 21<sup>st</sup> century were conducted under two  
309 Intergovernmental Panel on Climate Change (IPCC) climate scenarios (RCP 2.6 and RCP 8.5).  
310 The future climatic forcing data under these two climate change scenarios were derived from the  
311 HadGEM2-ESmodel, which is a member of CMIP5project213 ([https://esgf-](https://esgf-node.llnl.gov/search/cmip5/)  
312 [node.llnl.gov/search/cmip5/](https://esgf-node.llnl.gov/search/cmip5/)). Then the regional estimations were obtained by summing up the  
313 gridded outputs for our study region. The positive simulated NEP represents a CO<sub>2</sub> sink from the  
314 atmosphere to terrestrial ecosystems, while a negative value represents a source of CO<sub>2</sub> from  
315 terrestrial ecosystems to the atmosphere.

## 316 2.5 Parameter equifinality effects ~~uncertainty~~

317 Our previous studies using TEM has demonstrated that equifinality derived from site-level  
318 parameterization will affect the uncertainty in the estimation of regional carbon dynamics (Tang  
319 and Zhuang, 2008, 2009). Here equifinality refers to that a number of sets of parameters result in  
320 model simulations that all match the data similarly well. To quantify this e-effect on our simulation  
321 uncertainty, ~~parameter uncertainty in our model,~~ we conducted ensemble regional simulations with

322 50 sets of parameters for both historical and future studies. The 50 sets of parameters were obtained  
323 according to the method in Tang and Zhuang (2008).

### 324 3. Results

#### 325 3.1 Inversed Model Parameters and model validation

326 Using SCE-UA ensemble method, 50 independent sets of parameters were converged to  
327 minimize the objective function. Then the optimized parameters are calculated as the mean of these  
328 50 sets of inversed parameters. The boxplot of parameter posterior distributions reflects different  
329 ecosystem properties at these sites (Figure 3). For instance, growth yieldcarbon use efficiency  
330 (CUE) was much higher in tundra types than in forests, meaning microorganisms in environment  
331 with higher energy limitation tend to enhance the efficiency of energy transportation. Besides,  
332 alpha, the maintenance weight, was also much higher in tundra types than in forests. The opposite  
333 can be seen from the plot for parameter beta, the ratio of dormant maintenance rate to specific  
334 maintenance rate for active biomass in tundra types is lower than that in forest types. Other  
335 microbial related parameters did not differentiate much among different vegetation types.

336 After parameterization, the MIC-TEM-dormancy was validated with monthly NEP data for  
337 six representative ecosystems, and the comparisons between monthly observed NEP and  
338 simulated NEP were presented in Figure 4. With the optimized parameters, the dormancy-based  
339 model was used to reproduce NEP to compare with the measured NEP (Table 5). The statistical  
340 analysis shows that  $R^2$  ranges from 0.67 for Atqasuk to 0.93 for Bartlett Experimental Forest  
341 (Table 5). Generally, our new model performs better for forest ecosystems than for tundra  
342 ecosystems. Compared with MIC-TEM, which is no dormancy-based, dormancy model performs  
343 better for alpine tundra, temperate coniferous forest, and grassland. For other sites, both two  
344 models show similar performance (Table 5). Besides, a Another set of sites with monthly soil

345 respiration data were selected to ~~evaluate~~ ~~validate the ability of the estimated~~ ~~ing~~  $R_H$  of our  
346 ~~model~~ ~~conduct model validation~~. The comparisons between monthly observed  $R_H$  and simulated  
347  $R_H$  from two contrasting models were conducted (Figure 5). MIC-TEM-dormancy has higher  $R^2$   
348 and lower root mean square error (RMSE) (Table 6). Sixty-one sites with average annual  $R_H$  in  
349 northern high-latitude regions were used to further evaluate the new model performance. The  
350 dormancy model has lower intercept and slope with  $R^2$  of 0.45, while  $R^2$  of MIC-TEM is 0.3  
351 (Figure 6). These analyses indicate that new model is more realistic in representing ~~heterotrophic~~  
352 ~~respiration~~ ( $R_H$ ) by considering microbial dormancy. This difference ~~in~~  $R_H$  further affects soil  
353 available nitrogen dynamics, influencing nitrogen uptake by plants, the rate of photosynthesis  
354 and NPP (Zhuang et al., 2015; Zha et al., 2018; Thullner et al., 2005).

355

### 356 3.2 Regional carbon dynamics during the 20<sup>th</sup> century

357 Regional extrapolation with both models estimated a regional carbon sink but with different  
358 magnitudes (Figure 7c). ~~Here positive values of NEP represent sinks of CO<sub>2</sub> into terrestrial~~  
359 ~~ecosystems, while negative values represent sources of CO<sub>2</sub> to the atmosphere~~. With optimized  
360 parameters, MIC-TEM estimated a regional carbon sink of 77.6 Pg with the interannual standard  
361 deviation of 0.21 Pg C yr<sup>-1</sup> during the 20<sup>th</sup> century. However, MIC-TEM-dormancy nearly doubles  
362 the sink at 153.5 Pg with the interannual standard deviation of 0.12 Pg C yr<sup>-1</sup> during the last  
363 century, ~~which estimates 75.9 Pg more carbon sink than MIC-TEM does but with less interannual~~  
364 ~~variation~~ (Figure 7c). At the end of the century, MIC-TEM estimated that NEP reaches 1.0 Pg C  
365 yr<sup>-1</sup> in comparison with MIC-TEM-dormancy estimates of 1.5 Pg C yr<sup>-1</sup> (Figure 7c). Both models  
366 simulated similar trends for regional NPP,  $R_H$  and NEP (Figure 7). Generally, they show an  
367 increasing trend in the 20th century ~~except a slight decrease during the 1960s~~ (Figure 7).



368 Meanwhile, with optimized parameters, MIC-TEM-dormancy estimated NPP and  $R_H$  at 7.94 Pg C  
369  $\text{yr}^{-1}$  and 6.4 Pg C  $\text{yr}^{-1}$ , which are 5.8% and 16.3% less than the estimations from MIC-TEM,  
370 respectively (Figures 7a and 7b). This pronounced difference of NEP between two models comes  
371 from the disparity between the simulated NPP and  $R_H$  with them since NEP is calculated as the  
372 difference between NPP and  $R_H$ . Without considering dormancy, MIC-TEM estimates more active  
373 microbial biomass since it assumes the whole microbial biomass pool will participate in soil  
374 decomposition. The fact is only active part of microbial biomass can affect decompose organic  
375 matter decomposition~~work for soil decomposition~~, meaning MIC-TEM overestimates  $R_H$ . On the  
376 other hand, oOverestimation of  $R_H$  can induce higher nitrogen uptake by plants, which will  
377 accelerate rate of photosynthesis and further enhance NPP projection. Although MIC-TEM  
378 estimates higher NPP and  $R_H$  than MIC-TEM-dormancy does, NEP estimated from MIC-TEM is  
379 actually lower.

380 The average annual seasonal patterns of NPP,  $R_H$  and NEP during the 1990s were also  
381 organized from regional simulations with two models (Figure 8). Temporally, both ~~two~~ models  
382 projected higher NPP and  $R_H$  in summer than in winter (Figures 8a and 8b) due to higher soil  
383 temperature and moisture (McGuire et al., 1992). Setting the  $R_H$  projection from MIC-TEM as a  
384 baseline, MIC-TEM-dormancy averagely projected 33% less  $R_H$  in summer (May to September),  
385 and 30% more in winter (other months)~~MIC-TEM produced less  $R_H$  in winter but higher  $R_H$  in~~  
386 ~~summer than MIC-TEM dormancy~~ (Figure 8b), which indicates that without dormancy, model  
387 tends to estimate lower soil respiration compared to dormancy model due to ignorance of  
388 dormant respiration in winter but estimate higher soil respiration due to higher estimation of  
389 active biomass in summer. In the meantime, seasonal cycle of NPP with MIC-TEM-dormancy  
390 shows a relative flattening pattern compared with MIC-TEM, which is similar to seasonal cycle

391 of  $R_H$  (Figure 8a). ~~This is because higher  $R_H$  can cause higher NPP due to the reasons we have~~  
392 ~~mentioned above.~~ Though  $R_H$  and NPP show the similar seasonal patterns, NEP can still show  
393 different pattern ~~since it's the difference between NPP and  $R_H$ .~~ Here seasonal cycles of NEP with  
394 models are close to each other (Figure 8c), but dormancy model projected slightly higher NEP in  
395 summer. ~~Besides, setting the  $R_H$  projection from MIC-TEM as baseline, MIC-TEM dormancy~~  
396 ~~averagely projected 33% less  $R_H$  in summer (May to September), and 30% more in winter (other~~  
397 ~~months). This suggested that relative difference of  $R_H$  between two models in summer was~~  
398 ~~higher than in winter.~~

### 399 3.3 Regional carbon dynamics during the 21<sup>st</sup> century

400 Under the RCP 8.5 scenario, both models estimated the region acts as a carbon sink (Figure  
401 9). The MIC-TEM-dormancy predicted ~~a net C accumulation sequestration of 129.9 Pg by~~  
402 ~~the end of this century. that the sink is 129.9 Pg~~ with the interannual standard deviation of 0.13  
403 Pg C yr<sup>-1</sup>, whereas MIC-TEM estimates ~~a net C accumulation sequestration of 79.5 Pg the sink is~~  
404 ~~79.5 Pg~~ with the interannual standard deviation of 0.37 Pg C yr<sup>-1</sup> during the 21<sup>st</sup> century (Figure  
405 9). Thus, MIC-TEM-dormancy estimates an increase of 50.4 Pg regional carbon sequestration  
406 relative to MIC-TEM, ~~but~~ with less interannual variation (Figure 9). Under this scenario, both  
407 models predict similar temporal trends for NEP, namely increasing from the 2000s and then  
408 decreasing from the 2070s onward (Figure 9). MIC-TEM-dormancy predicts that carbon sink  
409 reaches 1.36 Pg C yr<sup>-1</sup> in the 2090s, which is 0.26 Pg C yr<sup>-1</sup> more than projection of MIC-TEM.  
410 Moreover, MIC-TEM-dormancy estimated NPP and  $R_H$  at 10.2 Pg C yr<sup>-1</sup> and 8.9 Pg C yr<sup>-1</sup>,  
411 which are 1.3 Pg C yr<sup>-1</sup> and 1.8 Pg C yr<sup>-1</sup> less than the estimations from MIC-TEM, respectively  
412 (Figure 9).

413 Under the RCP 2.6 scenario, the cumulative NEP from two models diverged by 125.2 Pg C  
414 by 2100. The trajectory of inter-annual NEP estimated with the two models also diverged. The  
415 MIC-TEM predicted the region fluctuates between carbon sinks and sources, and totally acts as a  
416 carbon source of 1.6 Pg C with the interannual standard deviation of 0.24 Pg C yr<sup>-1</sup> during the  
417 21<sup>st</sup> century. In contrast, MIC-TEM-dormancy projected the region acts as a carbon sink of 123.6  
418 Pg C with ~~an~~the interannual standard deviation of 0.1 Pg C yr<sup>-1</sup> (Figure 9). MIC-TEM-dormancy  
419 estimates NPP and R<sub>H</sub> at 9.9 Pg C yr<sup>-1</sup> and 8.7 Pg C yr<sup>-1</sup>, which are 0.5 Pg C yr<sup>-1</sup> and 1.7 Pg C yr<sup>-1</sup>  
420 <sup>1</sup> less than the estimations from MIC-TEM, respectively (Figure 9). Moreover, simulations under  
421 the two contrasting climate scenarios (RCP 2.6 and RCP 8.5) exhibit a large difference of 81.1  
422 Pg C of cumulative NEP during the 21<sup>st</sup> century by MIC-TEM, but only 6.3 Pg C of that by  
423 MIC-TEM-dormancy. This difference indicates microbes provide a resistant response to climate  
424 change due to dormancy to some extent (Treseder et al., 2011).  
425 The average annual seasonal patterns of NPP, R<sub>H</sub> and NEP during the 2990s by two models were  
426 also presented (Figure 10). MIC-TEM-dormancy estimated higher R<sub>H</sub> in winter, but lower R<sub>H</sub> in  
427 summer under both future scenarios (Figure 10). NPP is the same in winter with or without  
428 dormancy, and in the late summer is higher with than that without dormancy (i.e. opposite to  
429 R<sub>H</sub>), especially in the RCP 8.5 scenario. Similar seasonal cycle pattern appears for NPP  
430 projection. The combined flattening patterns of NPP and R<sub>H</sub> result in different patterns for NEP.  
431 Under the RCP 2.6 scenario, MIC-TEM-dormancy predicts higher NEP from June to October,  
432 but lower NEP from January to April compared similar NEP in other months to MIC-TEM  
433 (Figure 10). Under the RCP 8.5 scenario, MIC-TEM-dormancy predicts higher NEP from June  
434 to September, but much lower NEP in other months than MIC-TEM (Figure 10).

### 3.4 Regional uncertainty considering equifinality effects Ensemble simulations during for 20<sup>th</sup> and 21<sup>st</sup> centuries

The ensemble simulations for the 20<sup>th</sup> century is shown in Figure 11. Given the uncertainty in parameters, MIC-TEM-dormancy predicted that the regional cumulative carbon ranges from a carbon loss of 28.2 Pg to a carbon sink of 362.1 Pg by different ensemble members, with a mean of  $71.2 \pm 54.8$  Pg (Figure 11). For the 21<sup>st</sup> century, MIC-TEM-dormancy predicted that the region acts from a carbon source of 49.3 Pg C to a carbon sink of 296.5 Pg C, with a mean of  $112.7 \pm 116.5$  Pg under the RCP 2.6 scenario (Figure 12). Under the RCP 8.5 scenario, MIC-TEM-dormancy predicted that the region acts from a carbon source of 27.1 Pg C to a carbon sink of 401.3 Pg C, with a mean of  $143.1 \pm 162.5$  Pg (Figure 12).

## 4. Discussion

Soils are the largest carbon repository in the terrestrial biosphere and hold 2.5 times more carbon than the atmosphere (Frey et al., 2013; Schlesinger & Andrews, 2000). Especially, a significant portion of soil organic carbon ~~currently~~ stored in northern high latitudes ~~region~~ (Tarnocai et al., 2009). Besides, the magnitude of the warming in these regions is larger, almost twice, that of the global average climate over this region has warmed in recent decades (Serreze & Francis, 2006) and the changing climate is expected to alter the carbon cycle through influencing the activities of microorganisms in controlling soil decomposition (Manzoni et al., 2012; Melillo et al., 2011). Therefore, explicit consideration of microbial traits and functions in large-scale biogeochemistry models is necessary for better quantification of carbon-climate feedbacks (Thullner et al., 2005; Wang et al., 2015). Our regional simulations with two contrasting models (MIC-TEM, MIC-TEM-dormancy) indicate the region was a carbon sink in past decades, which is consistent with results from other process-based models (White et al.,

458 2000; Houghton et al., 2007; McGuire et al., 2009; Schimel, 2013). However, the magnitudes of  
459 this sink are quite different in two models. Moreover, MIC-TEM-dormancy predicts the sink will  
460 decrease under both RCP 8.5 and RCP 2.6 scenarios during the 21<sup>st</sup> century, while MIC-TEM  
461 projects that the sink will increase under the RCP 8.5 but change to carbon source under the RCP  
462 2.6 scenario. Estimations based on models without dormancy could fit observations of  $R_H$  as well  
463 as estimations with dormancy, but at the cost of underestimating microbial biomass (Wang et al.,  
464 2014). Differences in predicted  $R_H$  with and without dormancy increase with temperature and  
465 with the length of the dry periods between wetting events (Salazar et al., 2018). The large  
466 difference in two models suggests the importance of incorporating microbial dormancy effects.

467 The large bias between dormancy and non-dormancy models mainly comes from two parts.  
468 First, ~~many-most~~ important microbial activities such as soil organic carbon decomposition and  
469 nutrient cycling largely depend on the active fraction of microbial communities, not total  
470 microbial biomass (Wang et al., 2014; Blagodatsky et al., 2000). However, only a small part  
471 (about 0.1-2%, seldom exceed 5%) of the total soil microbial biomass is recognized to be active  
472 under natural conditions (Blagodatsky et al., 2011; Werf & Verstraete, 1987). Thus, dormancy  
473 could be a prominent feature in soil systems (Wang et al., 2014). Without considering dormancy,  
474 the “effective” microbial biomass for soil decomposition could be overestimated, resulting in  
475 overestimation of heterotrophic respiration (He et al., 2015). ~~Our regional estimate of  $R_H$  is 6.4~~  
476 ~~Pg C yr<sup>-1</sup> during the 20<sup>th</sup> century by MIC-TEM dormancy, while 7.7 Pg C yr<sup>-1</sup> by MIC-TEM. No~~  
477 ~~dormancy model simulated 20.3% higher respiration than dormancy model. For future~~  
478 ~~simulations, MIC-TEM dormancy predicted 8.7 Pg C yr<sup>-1</sup> and 9.0 Pg C yr<sup>-1</sup> of  $R_H$  under RCP 2.6~~  
479 ~~and RCP 8.5 scenarios during the 21<sup>st</sup> century, respectively. Nevertheless, no dormancy model~~  
480 ~~simulated 19.5% and 21.2% higher respiration than dormancy model under RCP 2.6 and RCP 8.5~~

481 ~~scenarios, respectively.~~ He et al. (2015) predicted total soil  $R_H$  of all temperate forests (25°N-  
482 50°N) from the dormancy model amounted to 7.28 Pg C yr<sup>-1</sup> and 8.83 Pg C yr<sup>-1</sup> from a no-  
483 dormancy model, which is 21.3% higher than the dormancy model. Although their study region  
484 and simulation period are different from our study, the results can still be comparable. Both  
485 studies indicated that the magnitude of  $R_H$  ~~and proportion~~ from no-dormancy model are higher  
486 than dormancy models. Second, high soil respiration stimulates N mineralization in soils  
487 (Zhuang et al., 2001, 2002), making more nutrients for photosynthesis of plants (Raich et al.,  
488 1991; McGuire et al., 1995). Therefore, NPP will be higher due to the N enrichment from higher  
489  $R_H$ . However, how NEP will change is still unclear. ~~Our regional estimate of NEP during the 20<sup>th</sup>~~  
490 ~~century by MIC-TEM dormancy is 1.54 Pg C yr<sup>-1</sup>, and is 0.78 Pg C yr<sup>-1</sup> by MIC-TEM. Our~~  
491 ~~estimates of the northern extratropical NEP in the 1980s (1.61 Pg C yr<sup>-1</sup> with MIC-TEM-~~  
492 ~~dormancy and 0.84 Pg C yr<sup>-1</sup> with MIC-TEM) are within ranges (0.6 to 2.3 PgC yr<sup>-1</sup>) reported in~~  
493 ~~the literature for northern regions (Schimel et al., (2001), reported that a range of estimates of the~~  
494 ~~northern extratropical NEP is from 0.6 to 2.3 PgC yr<sup>-1</sup> in the 1980s. In comparison with our~~  
495 ~~estimates of 1.61 Pg C yr<sup>-1</sup> with MIC-TEM dormancy and 0.84 Pg C yr<sup>-1</sup> with MIC-TEM, our~~  
496 ~~regional estimates of NEP are in reasonable range.~~ Moreover, our predicted time trajectory trend  
497 of NEP in the 21<sup>st</sup> century under the RCP 2.6 scenario is very similar to the finding of White et  
498 al. (2000), indicating that NEP increases from the 2000s to the 2070s, and then decreases in the  
499 2090s. ~~Moreover, future simulations under two contrasting climate scenarios (RCP 2.6 and RCP~~  
500 ~~8.5) exhibit a large difference of 81.1 Pg C of cumulative NEP during the 21<sup>st</sup> century by MIC-~~  
501 ~~TEM, but only 6.3 Pg C of that by MIC-TEM dormancy. This difference indicates microbes~~  
502 ~~provide a resistant response to climate change due to dormancy to some extent (Treseder et al.,~~  
503 ~~2011).~~

504 Although our dormancy model can project reasonable carbon fluxes and indicate the  
505 importance of incorporating microbial dormancy when compared with ~~MIC-TEM~~  
506 ~~model~~ (Zha & Zhuang et al., 2018), there are some other microbial traits have not yet  
507 been considered in our model. For instance, one vital common evolutionary trait of microbe is  
508 the community shift (Wang et al., 2015) with changing environment, including warming, N  
509 fertilization and precipitation (Treseder et al., 2011; Frey et al., 2013; Allison et al., 2009; Evans  
510 & Wallenstein, 2011). Community shift will influence microbial physiology, temperature  
511 sensitivity and growth rates (Classen et al., 2015), which will further affect the rate of soil  
512 decomposition and other carbon dynamics (Treseder et al., 2011; Schimel & Schaeffer, 2012;  
513 Todd-Brown et al., 2011). ~~Moreover, microbial acclimation is another important trait to affect~~  
514 ~~soil decomposition. Recent studies have found the capacity of the microbial community to~~  
515 ~~maintain the warming-induced elevated respiration could decrease over time because of~~  
516 ~~acclimation (Melillo et al. 1993; Todd-Brown et al., 2011). This mechanism of adaption to a new~~  
517 ~~temperature regime shall be factored into future soil decomposition analysis.~~ Besides, microbial  
518 community composition was ignored in our model. We didn't separate among functional  
519 microbial groups, but gather microbes into one "box". However, microbial community  
520 composition could influence ecosystem functioning, and their variance in responses to  
521 environmental conditions could alter the prediction of the rates of decomposition of organic  
522 material (Balsler et al. 2002; Fierer et al. 2007). Especially, some narrowly-distributed functions  
523 can be more sensitive to microbial community composition, and these might benefit most from  
524 explicit consideration of distinguishing functional groups in ecosystem models (McGuire &  
525 Treseder, 2010; Schimel 1995). Thus, functional dissimilarity in microbial communities can be  
526 considered in next step for model development (Strickland et al., 2009; Moorhead et al., 2006).

527 Moreover, microbial acclimation, a mechanism of adaption to a new temperature regime, is  
528 another important trait to affect soil decomposition. Recent studies have found that the warming-  
529 induced elevated respiration of the microbial community could decrease over time because of  
530 acclimation (Melillo et al. 1993; Todd-Brown et al., 2011). This mechanism shall be factored  
531 into future soil decomposition analysis.

532 Except for model limitations mentioned above~~above model limitations~~, additional  
533 uncertainties may come from inadequate model parameterization and model assumptions. For  
534 example, a critical microbial parameter, carbon use efficiency (CUE), is a primary control to soil  
535 CO<sub>2</sub> efflux. Higher CUE indicates more microbial growth and more carbon uptake by plants,  
536 while lower CUE indicates higher soil decomposition (Manzoni et al., 2012). Theoretical and  
537 empirical studies have suggested that CUE depends on both temperature and substrate quality  
538 (Frey et al., 2013) and decreases as temperature increases and nutrient availability decreases  
539 (Manzoni et al., 2012). Our study considered the CUE sensitivity to temperature, but not nutrient  
540 availability. On the other hand, some model assumptions can also cause uncertainties. For  
541 example, we assumed that vegetation will not change during the transient simulation. However,  
542 over the past few decades in northern high latitudes, temperature increases have led to vegetation  
543 shift from one type to another (Hansen et al., 2006; White et al., 2000). The vegetation changes  
544 will affect carbon cycling in these ecosystems.

545

## 546 **5. Conclusions**

547 This study incorporated microbial dormancy into a detailed microbial-based soil  
548 decomposition biogeochemistry model to examine the fate of large Arctic soil carbon under  
549 changing climate conditions. Regional simulations using MIC-TEM-dormancy indicated that,



550 over the 20<sup>th</sup> century, the region is a carbon sink of 153.5 Pg. This sink could decrease to 129.9  
551 Pg under the RCP 8.5 scenario or 123.6 Pg under the RCP 2.6 scenario during the 21<sup>st</sup> century.  
552 Whether considering microbial dormancy or not can cause large differences in soil  
553 decomposition estimation between two models. Meanwhile, due to available nitrogen affected by  
554 soil decomposition, net primary production is consequently influenced in these two centuries.  
555 The combined changes in soil decomposition and net primary production led to large differences  
556 in carbon budget estimation between two models. Compared with MIC-TEM, MIC-TEM-  
557 dormancy projected 75.9 Pg more C stored in the terrestrial ecosystems over the last century,  
558 50.4 Pg and 125.2 Pg more C under the RCP 8.5 and RCP 2.6 scenarios, respectively. This study  
559 highlights the importance of the representation of microbial dormancy in earth system models in  
560 order to adequately quantify the carbon dynamics in northern high latitudes.

561

## 562 **Acknowledgments**

563 This research was supported by a NSF project (IIS-1027955), a DOE project (DE-SC0008092),  
564 and a NASA LCLUC project (NNX09AI26G) to Q. Z. We acknowledge the Rosen High  
565 Performance Computing Center at Purdue for computing support. We thank the National Snow  
566 and Ice Data center for providing Global Monthly EASE-Grid Snow Water Equivalent data,  
567 National Oceanic and Atmospheric Administration for North American Regional Reanalysis  
568 (NARR). We also acknowledge the World Climate Research Programme's Working Group on  
569 Coupled Modeling Intercomparison Project CMIP5, and we thank the climate modeling groups  
570 for producing and making available their model output. The data presented in this paper can be  
571 accessed through our research website (<http://www.eaps.purdue.edu/ebdl/>)

572

573

574 **References:**

- 575 Allison, E. H., Perry, A. L., Badjeck, M.-C., Neil Adger, W., Brown, K., Conway, D., Halls, A.  
576 S., Pilling, G. M., Reynolds, J. D., Andrew, N. L., and Dulvy, N. K.: Vulnerability of national  
577 economies to the impacts of climate change on fisheries, *Fish and Fisheries*, 10, 173-196,  
578 10.1111/j.1467-2979.2008.00310.x, 2009.
- 579 Allison, S. D., Wallenstein, M. D., and Bradford, M. A.: Soil-carbon response to warming  
580 dependent on microbial physiology, *Nature Geoscience*, 3, 336-340, 10.1038/ngeo846, 2010.
- 581 Balser, T. C., Kinzig, A. P., and Firestone, M. K.: Linking soil microbial communities and  
582 ecosystem functioning, *The functional consequences of biodiversity: Empirical progress and*  
583 *theoretical extensions*, 265-293, 2002.
- 584 Blagodatskaya, E., and Kuzyakov, Y.: Active microorganisms in soil: Critical review of  
585 estimation criteria and approaches, *Soil Biology and Biochemistry*, 67, 192-211,  
586 10.1016/j.soilbio.2013.08.024, 2013.
- 587 Blagodatskaya, E., Khomyakov, N., Myachina, O., Bogomolova, I., Blagodatsky, S., and  
588 Kuzyakov, Y.: Microbial interactions affect sources of priming induced by cellulose, *Soil*  
589 *Biology and Biochemistry*, 74, 39-49, 10.1016/j.soilbio.2014.02.017, 2014.
- 590 Blagodatsky, S., Grote, R., Kiese, R., Werner, C., and Butterbach-Bahl, K.: Modelling of  
591 microbial carbon and nitrogen turnover in soil with special emphasis on N-trace gases emission,  
592 *Plant and soil*, 346, 297-330, 10.1007/s11104-011-0821-z, 2011.
- 593 Blagodatsky, S. A., Heinemeyer, O., and Richter, J.: Estimating the active and total soil  
594 microbial biomass by kinetic respiration analysis, *Biol Fertil Soils*, 32, 73-81, 2000.
- 595 Bond-Lamberty, B., and Thomson, A.: Temperature-associated increases in the global soil  
596 respiration record, *Nature*, 464, 579-582, 10.1038/nature08930, 2010.
- 597 Bond-Lamberty, B., Bailey, V. L., Chen, M., Gough, C. M., and Vargas, R.: Globally rising soil  
598 heterotrophic respiration over recent decades, *Nature*, 560, 80-83, 10.1038/s41586-018-0358-x,  
599 2018.
- 600 Bouskill, N. J., Tang, J., Riley, W. J., and Brodie, E. L.: Trait-based representation of biological  
601 nitrification: model development, testing, and predicted community composition, *Frontiers in*  
602 *microbiology*, 3, 364, 10.3389/fmicb.2012.00364, 2012.
- 603 Callaghan, T., Björn, L. O., Chernov, Y., Chapin, T., Christensen, T. R., Huntley, B., Ims, R.,  
604 Jolly, D., Jonasson, S., Matveyeva, N., Panikov, N., Oechel, W., and Shaver, G.: Arctic tundra  
605 and polar desert ecosystems, *Arctic climate impact assessment*, 243-352, 2005.
- 606 Carney, K. M., and Matson, P. A.: The influence of tropical plant diversity and composition on  
607 soil microbial communities, *Microbial ecology*, 52, 226-238, 10.1007/s00248-006-9115-z, 2006.
- 608 Chmielewski, R. A. N., and Frank, J. F.: Formation of viable but nonculturable *Salmonella*  
609 during starvation in chemically defined solutions, *Letters in Applied Microbiology*, 20, 380-384,  
610 1995.
- 611 Classen, A. T., Sundqvist, M. K., Henning, J. A., Newman, G. S., Moore, J. A. M., Cregger, M.  
612 A., Moorhead, L. C., and Patterson, C. M.: Direct and indirect effects of climate change on soil  
613 microbial and soil microbial-plant interactions: What lies ahead?, *Ecosphere*, 6, art130,  
614 10.1890/es15-00217.1, 2015.
- 615 Conant, R. T., Ryan, M. G., Ågren, G. I., Birge, H. E., Davidson, E. A., Eliasson, P. E., Evans, S.  
616 E., Frey, S. D., Giardina, C. P., Hopkins, F. M., Hyvönen, R., Kirschbaum, M. U. F., Lavallee, J.  
617 M., Leifeld, J., Parton, W. J., Megan Steinweg, J., Wallenstein, M. D., Martin Wetterstedt, J. Å.,  
618 and Bradford, M. A.: Temperature and soil organic matter decomposition rates - synthesis of

619 current knowledge and a way forward, *Global change biology*, 17, 3392-3404, 10.1111/j.1365-  
620 2486.2011.02496.x, 2011.

621 Coursolle, C., Margolis, H. A., Barr, A. G., Black, T. A., Amiro, B. D., McCaughey, J. H.,  
622 Flanagan, L. B., Lafleur, P. M., Roulet, N. T., Bourque, C. P. A., Arain, M. A., Wofsy, S. C.,  
623 Dunn, A., Morgenstern, K., Orchansky, A. L., Bernier, P. Y., Chen, J. M., Kidston, J., Saigusa,  
624 N., and Hedstrom, N.: Late-summer carbon fluxes from Canadian forests and peatlands along an  
625 east–west continental transect, *Canadian Journal of Forest Research*, 36, 783-800, 10.1139/x05-  
626 270, 2006.

627 Davidson, E. A., Trumbore, S. E., and Amundson, R.: Biogeochemistry: soil warming and  
628 organic carbon content, *Nature*, 408, 2000.

629 Davidson, E. A., and Janssens, I. A.: Temperature sensitivity of soil carbon decomposition and  
630 feedbacks to climate change, *Nature*, 440, 165-173, 10.1038/nature04514, 2006.

631 Davidson, E. A., Janssens, I. A., and Luo, Y.: On the variability of respiration in terrestrial  
632 ecosystems: moving beyond Q<sub>10</sub>, *Global change biology*, 12, 154-164, 10.1111/j.1365-  
633 2486.2005.01065.x, 2006.

634 Davidson, E. A., Samanta, S., Caramori, S. S., and Savage, K.: The Dual Arrhenius and  
635 Michaelis-Menten kinetics model for decomposition of soil organic matter at hourly to seasonal  
636 time scales, *Global change biology*, 18, 371-384, 10.1111/j.1365-2486.2011.02546.x, 2012.

637 Duan, Q., Sorooshian, S., and Gupta, V. K.: Optimal use of the SCE-UA global optimization  
638 method for calibrating watershed models, *Journal of Hydrology*, 158, 265-284, 1994.

639 Evans, S. E., and Wallenstein, M. D.: Soil microbial community response to drying and  
640 rewetting stress: does historical precipitation regime matter?, *Biogeochemistry*, 109, 101-116,  
641 10.1007/s10533-011-9638-3, 2011.

642 Fierer, N., Morse, J. L., Berthrong, S. T., Bernhardt, E. S., and Jackson, R. B.: Environmental  
643 controls on the landscape - scale biogeography of stream bacterial communities, *Ecology*, 88,  
644 2162-2173, 2007.

645 Frey, S. D., Lee, J., Melillo, J. M., and Six, J.: The temperature response of soil microbial  
646 efficiency and its feedback to climate, *Nature Climate Change*, 3, 395-398,  
647 10.1038/nclimate1796, 2013.

648 ~~Gangsheng Wang, M. A. M., Lianhong Gu, Christopher W. Schadt: Representation of Dormant~~  
649 ~~and Active Microbial Dynamics for Ecosystem Modeling, *Public Library of Science*, 9,~~  
650 ~~10.1371/journal.pone.0089252.g001, 2014.~~

651 German, D. P., Marcelo, K. R. B., Stone, M. M., and Allison, S. D.: The Michaelis-Menten  
652 kinetics of soil extracellular enzymes in response to temperature: a cross-latitudinal study,  
653 *Global change biology*, 18, 1468-1479, 10.1111/j.1365-2486.2011.02615.x, 2012.

654 Gilmanov, T. G., Tieszen, L. L., Wylie, B. K., Flanagan, L. B., Frank, A. B., Haferkamp, M. R.,  
655 Meyers, T. P., and Morgan, J. A.: Integration of CO<sub>2</sub> flux and remotely-sensed data for primary  
656 production and ecosystem respiration analyses in the Northern Great Plains: potential for  
657 quantitative spatial extrapolation, *Global Ecology and Biogeography*, 14, 271-292,  
658 10.1111/j.1466-822X.2005.00151.x, 2005.

659 Gough, C. M., Hardiman, B. S., Nave, L. E., Bohrer, G., Maurer, K. D., Vogel, C. S.,  
660 Nadelhoffer, K. J., and Curtis, P. S.: Sustained carbon uptake and storage following moderate  
661 disturbance in a Great Lakes forest, *Ecological Applications*, 23, 1202-1215, 2013.

662 Goulden, M. L., Winston, G. C., McMillan, A. M. S., Litvak, M. E., Read, E. L., Rocha, A. V.,  
663 and Rob Elliot, J.: An eddy covariance mesonet to measure the effect of forest age on

664 land?atmosphere exchange, *Global change biology*, 12, 2146-2162, 10.1111/j.1365-  
665 2486.2006.01251.x, 2006.

666 Graham, E. B., Wieder, W. R., Leff, J. W., Weintraub, S. R., Townsend, A. R., Cleveland, C. C.,  
667 Philippot, L., and Nemergut, D. R.: Do we need to understand microbial communities to predict  
668 ecosystem function? A comparison of statistical models of nitrogen cycling processes, *Soil*  
669 *Biology and Biochemistry*, 68, 279-282, 10.1016/j.soilbio.2013.08.023, 2014.

670 Graham, E. B., Knelman, J. E., Schindlbacher, A., Siciliano, S., Breulmann, M., Yannarell, A.,  
671 Beman, J. M., Abell, G., Philippot, L., Prosser, J., Foulquier, A., Yuste, J. C., Glanville, H. C.,  
672 Jones, D. L., Angel, R., Salminen, J., Newton, R. J., Burgmann, H., Ingram, L. J., Hamer, U.,  
673 Siljanen, H. M., Peltoniemi, K., Potthast, K., Baneras, L., Hartmann, M., Banerjee, S., Yu, R. Q.,  
674 Nogaro, G., Richter, A., Koranda, M., Castle, S. C., Goberna, M., Song, B., Chatterjee, A.,  
675 Nunes, O. C., Lopes, A. R., Cao, Y., Kaisermann, A., Hallin, S., Strickland, M. S., Garcia-  
676 Pausas, J., Barba, J., Kang, H., Isobe, K., Papaspyrou, S., Pastorelli, R., Lagomarsino, A.,  
677 Lindstrom, E. S., Basiliko, N., and Nemergut, D. R.: Microbes as Engines of Ecosystem  
678 Function: When Does Community Structure Enhance Predictions of Ecosystem Processes?,  
679 *Frontiers in microbiology*, 7, 214, 10.3389/fmicb.2016.00214, 2016.

680 Griffis, T. J., Lee, X., Baker, J. M., Billmark, K., Schultz, N., Erickson, M., Zhang, X.,  
681 Fassbinder, J., Xiao, W., and Hu, N.: Oxygen isotope composition of evapotranspiration and its  
682 relation to C<sub>4</sub>photosynthetic discrimination, *Journal of Geophysical Research*, 116,  
683 10.1029/2010jg001514, 2011.

684 Hagerty, S. B., van Groenigen, K. J., Allison, S. D., Hungate, B. A., Schwartz, E., Koch, G. W.,  
685 Kolka, R. K., and Dijkstra, P.: Accelerated microbial turnover but constant growth efficiency  
686 with warming in soil, *Nature Climate Change*, 4, 903-906, 10.1038/nclimate2361, 2014.

687 Hansen, J., Sato, M., Ruedy, R., Lo, K., Lea, D. W., and Medina-Elizade, M.: Global  
688 temperature change, *Proceedings of the National Academy of Sciences of the United States of*  
689 *America*, 103, 14288-14293, 10.1073/pnas.0606291103, 2006.

690 Harder, w., and Dijkhuizen, L.: Physiological responses to nutrient limitation, *Annual Review of*  
691 *Microbiology*, 37, 1983.

692 Harris, I., Jones, P. D., Osborn, T. J., and Lister, D. H.: Updated high-resolution grids of monthly  
693 climatic observations - the CRU TS3.10 Dataset, *International Journal of Climatology*, 34, 623-  
694 642, 10.1002/joc.3711, 2014.

695 He, Y., Yang, J., Zhuang, Q., Harden, J. W., McGuire, A. D., Liu, Y., Wang, G., and Gu, L.:  
696 Incorporating microbial dormancy dynamics into soil decomposition models to improve  
697 quantification of soil carbon dynamics of northern temperate forests, *Journal of Geophysical*  
698 *Research: Biogeosciences*, 120, 2596-2611, 10.1002/2015jg003130, 2015.

699 Hiller, R. V., McFadden, J. P., and Kljun, N.: Interpreting CO<sub>2</sub> Fluxes Over a Suburban Lawn:  
700 The Influence of Traffic Emissions, *Boundary-Layer Meteorology*, 138, 215-230,  
701 10.1007/s10546-010-9558-0, 2010.

702 Houghton, R. A.: Balancing the Global Carbon Budget, *Annual Review of Earth and Planetary*  
703 *Sciences*, 35, 313-347, 10.1146/annurev.earth.35.031306.140057, 2007.

704 Hugelius, G., Strauss, J., Zubrzycki, S., Harden, J. W., Schuur, E. A. G., Ping, C. L.,  
705 Schirmermeister, L., Grosse, G., Michaelson, G. J., Koven, C. D., amp, apos, Donnell, J. A.,  
706 Elberling, B., Mishra, U., Camill, P., Yu, Z., Palmtag, J., and Kuhry, P.: Estimated stocks of  
707 circumpolar permafrost carbon with quantified uncertainty ranges and identified data gaps,  
708 *Biogeosciences*, 11, 6573-6593, 10.5194/bg-11-6573-2014, 2014.

709 Jenkins, J. P., Richardson, A. D., Braswell, B. H., Ollinger, S. V., Hollinger, D. Y., and Smith,  
710 M. L.: Refining light-use efficiency calculations for a deciduous forest canopy using  
711 simultaneous tower-based carbon flux and radiometric measurements, *Agricultural and Forest*  
712 *Meteorology*, 143, 64-79, 10.1016/j.agrformet.2006.11.008, 2007.

713 Kaiser, C., Franklin, O., Dieckmann, U., and Richter, A.: Microbial community dynamics  
714 alleviate stoichiometric constraints during litter decay, *Ecology letters*, 17, 680-690,  
715 10.1111/ele.12269, 2014.

716 Knorr, W., Prentice, I. C., House, J. I., and Holland, E. A.: Long-term sensitivity of soil carbon  
717 turnover to warming, *Nature*, 433, 2005.

718 Lawrence, C. R., Neff, J. C., and Schimel, J. P.: Does adding microbial mechanisms of  
719 decomposition improve soil organic matter models? A comparison of four models using data  
720 from a pulsed rewetting experiment, *Soil Biology and Biochemistry*, 41, 1923-1934,  
721 10.1016/j.soilbio.2009.06.016, 2009.

722 Lennon, J. T., and Jones, S. E.: Microbial seed banks: the ecological and evolutionary  
723 implications of dormancy, *Nature reviews. Microbiology*, 9, 119-130, 10.1038/nrmicro2504,  
724 2011.

725 Lloyd, A. H., Rupp, T. S., Fastie, C. L., and Starfield, A. M.: Patterns and dynamics of treeline  
726 advance on the Seward Peninsula, Alaska, *Journal of Geophysical Research*, 108,  
727 10.1029/2001jd000852, 2002.

728 Manzoni, S., Taylor, P., Richter, A., Porporato, A., and Agren, G. I.: Environmental and  
729 stoichiometric controls on microbial carbon-use efficiency in soils, *The New phytologist*, 196,  
730 79-91, 10.1111/j.1469-8137.2012.04225.x, 2012.

731 McEwing, K. R., Fisher, J. P., and Zona, D.: Environmental and vegetation controls on the  
732 spatial variability of CH<sub>4</sub> emission from wet-sedge and tussock tundra ecosystems in the Arctic,  
733 *Plant and soil*, 388, 37-52, 10.1007/s11104-014-2377-1, 2015.

734 McGuire, A. D., Melillo, J. M., Joyce, L. A., Kicklighter, D. W., Grace, A. L., III, B. M., and  
735 Vorosmarty, C. J.: Interactions between carbon and nitrogen dynamics in estimating net primary  
736 productivity for potential vegetation in North America, *Global Biogeochemical Cycles*, 6, 101-  
737 124, 1992.

738 McGuire, A. D., Melillo, J. M., Kicklighter, D. W., and Joyce, L. A.: Equilibrium responses of  
739 soil carbon to climate change: Empirical and process-based estimates, *Journal of Biogeography*,  
740 22, 785-796, 1995.

741 McGuire, A. D., and Hobbie, J. E.: Global climate change and the equilibrium responses of  
742 carbon storage in arctic and subarctic regions, In *Modeling the Arctic system: A workshop report*  
743 *on the state of modeling in the Arctic System Science program*, 53-54, 1997.

744 McGuire, A. D., Anderson, L. G., Christensen, T. R., Dallimore, S., Guo, L., Hayes, D. J.,  
745 Heimann, M., Lorenson, T. D., Macdonald, R. W., and Roulet, N.: Sensitivity of the carbon  
746 cycle in the Arctic to climate change, *Ecological Monographs*, 79, 523-555, 2009.

747 McGuire, K. L., and Treseder, K. K.: Microbial communities and their relevance for ecosystem  
748 models: Decomposition as a case study, *Soil Biology and Biochemistry*, 42, 529-535,  
749 10.1016/j.soilbio.2009.11.016, 2010.

750 Me´tris, A., Gerrard, A. M., Cumming, R. H., Weigner, P., and Paca, J.: Modelling shock  
751 loadings and starvation in the biofiltration of toluene and xylene, *Journal of Chemical*  
752 *Technology and Biotechnology*, 76, 565-572, 2001.

753 Melillo, J. M., McGuire, A. D., Kicklighter, D. W., III, B. M., Vorosmarty, C. J., and Schloss, A.  
754 L.: Global climate change and terrestrial net primary production, *Nature*, 363, 1993.

755 Melillo, J. M., Butler, S., Johnson, J., Mohan, J., Steudler, P., Lux, H., Burrows, E., Bowles, F.,  
756 Smith, R., Scott, L., Vario, C., Hill, T., Burton, A., Zhou, Y.-M., and Tang, J.: Soil warming,  
757 carbon - nitrogen interactions, and forest carbon budgets, *PNAS*, 108, 9508-9512, 2011.  
758 Merbold, L., Kutsch, W. L., Corradi, C., Kolle, O., Rebmann, C., Stoy, P. C., Zimov, S. A., and  
759 Schulze, E. D.: Artificial drainage and associated carbon fluxes (CO<sub>2</sub>/CH<sub>4</sub>) in a tundra  
760 ecosystem, *Global change biology*, 15, 2599-2614, 10.1111/j.1365-2486.2009.01962.x, 2009.  
761 Moorhead, D. L., and Sinsabaugh, R. L.: A theoretical model of litter decay and microbial  
762 interaction, *Ecological Monographs*, 76, 151-174, 2006.  
763 Oechel, W. C., Laskowski, C. A., Burba, G., Gioli, B., and Kalhori, A. A. M.: Annual patterns  
764 and budget of CO<sub>2</sub> flux in an Arctic tussock tundra ecosystem, *Journal of Geophysical Research:*  
765 *Biogeosciences*, 119, 323-339, 10.1002/2013jg002431, 2014.  
766 P.J. Hanson, N. T. E., C.T. Garten, J.A. Andrews: Separating root and soil microbial  
767 contributions to soil respiration: A review of methods and observations, *Biogeochemistry*, 48,  
768 115-146, 2000.  
769 Parton, W. J., Scurlock, J. M. O., Ojima, D. S., Gilmanov, T. G., Scholes, R. J., Schimel, D. S.,  
770 Kirchner, T., Menaut, J. C., Seastedt, T., Moya, E. G., Kamnalrut, A., and Kinyamario, J. I.:  
771 Observations and modeling of biomass and soil organic matter dynamics for the grassland biome  
772 worldwide, *Global Biogeochemical Cycles*, 7, 785-809, 1993.  
773 Raich, J. W., Rastetter, E. B., Melillo, J. M., Kicklighter, D. W., Steudler, P. A., Peterson, B. J.,  
774 Grace, A. L., III, B. M., and Vorosmarty, C. J.: Potential net primary productivity in South  
775 America: application of a global model, *Ecological Applications*, 1, 399-429, 1991.  
776 Richardson, A. D., Jenkins, J. P., Braswell, B. H., Hollinger, D. Y., Ollinger, S. V., and Smith,  
777 M. L.: Use of digital webcam images to track spring green-up in a deciduous broadleaf forest,  
778 *Oecologia*, 152, 323-334, 10.1007/s00442-006-0657-z, 2007.  
779 Running, S. W., and Coughlan, J. C.: A general model of forest ecosystem processes for regional  
780 applications I. Hydrologic balance, canopy gas exchange and primary production processes.,  
781 *Ecological Modelling*, 42, 125-154, 1988.  
782 Schimel, D. S.: Terrestrial ecosystems and the carbon cycle, *Global change biology*, 1, 77-91,  
783 1995.  
784 Schimel, D. S., House, J. I., Hibbard, K. A., Bousquet, P., Ciais, P., Peylin, P., Braswell, B. H.,  
785 Apps, M. J., Baker, D., Bondeau, A., Canadell, J., Churkina, G., Cramer, W., Denning, A. S.,  
786 Field, C. B., Friedlingstein, P., Goodale, C., Heimann, M., Houghton, R. A., Melillo, J. M., III,  
787 B. M., Murdiyarso, D., Noble, I., Pacala, S. W., Prentice, I. C., Raupach, M. R., Rayner, P. J.,  
788 Scholes, R. J., Steffen, W. L., and Wirth, C.: Recent patterns and mechanisms of carbon  
789 exchange by terrestrial ecosystems, *Nature*, 414, 2001.  
790 Schimel, J.: Microbes and global carbon, *Nature Climate Change*, 3, 867-868,  
791 10.1038/nclimate2015, 2013.  
792 Schimel, J. P., and Weintraub, M. N.: The implications of exoenzyme activity on microbial  
793 carbon and nitrogen limitation in soil: a theoretical model, *Soil Biology and Biochemistry*, 35,  
794 549-563, 10.1016/s0038-0717(03)00015-4, 2003.  
795 Schimel, J. P., and Schaeffer, S. M.: Microbial control over carbon cycling in soil, *Frontiers in*  
796 *microbiology*, 3, 348, 10.3389/fmicb.2012.00348, 2012.  
797 Schlesinger, W. H., and Andrews, J. A.: Soil respiration and the global carbon cycle,  
798 *Biogeochemistry*, 48, 7-20, 2000.  
799 Schmidt, M. W., Torn, M. S., Abiven, S., Dittmar, T., Guggenberger, G., Janssens, I. A., Kleber,  
800 M., Kogel-Knabner, I., Lehmann, J., Manning, D. A., Nannipieri, P., Rasse, D. P., Weiner, S.,

801 and Trumbore, S. E.: Persistence of soil organic matter as an ecosystem property, *Nature*, 478,  
802 49-56, 10.1038/nature10386, 2011.

803 Serreze, M. C., and Francis, J. A.: The Arctic on the fast track of change, *Weather*, 61, 65-69,  
804 2006.

805 Stolpovsky, K., Martinez-Lavanchy, P., Heipieper, H. J., Van Cappellen, P., and Thullner, M.:  
806 Incorporating dormancy in dynamic microbial community models, *Ecological Modelling*, 222,  
807 3092-3102, 10.1016/j.ecolmodel.2011.07.006, 2011.

808 Stow, D. A., Hope, A., McGuire, D., Verbyla, D., Gamon, J., Huemmrich, F., Houston, S.,  
809 Racine, C., Sturm, M., Tape, K., Hinzman, L., Yoshikawa, K., Tweedie, C., Noyle, B.,  
810 Silapaswan, C., Douglas, D., Griffith, B., Jia, G., Epstein, H., Walker, D., Daeschner, S.,  
811 Petersen, A., Zhou, L., and Myneni, R.: Remote sensing of vegetation and land-cover change in  
812 Arctic Tundra Ecosystems, *Remote Sensing of Environment*, 89, 281-308,  
813 10.1016/j.rse.2003.10.018, 2004.

814 Strickland, M. S., Lauber, C., Fierer, N., and Bradford, M. A.: Testing the functional  
815 significance of microbial community composition, *Ecology*, 90, 441-451, 2009.

816 [Tang, J., Q. Zhuang \(2009\) A global sensitivity analysis and Bayesian inference framework for  
817 improving the parameter estimation and prediction of a process-based Terrestrial Ecosystem  
818 Model J. Geophys. Res., 114, D15303, doi:10.1029/2009JD011724., 2009.](#)

819 [Tang, J., Q. Zhuang \(2008\) Equifinality in parameterization of process-based biogeochemistry  
820 models: A significant uncertainty source to the estimation of regional carbon dynamics J.  
821 Geophys. Res., 113, G04010, doi:10.1029/2008JG000757, 2008.](#)

822 Tang, J., and Riley, W. J.: Weaker soil carbon–climate feedbacks resulting from microbial and  
823 abiotic interactions, *Nature Climate Change*, 5, 56-60, 10.1038/nclimate2438, 2014.

824 Tape, K. E. N., Sturm, M., and Racine, C.: The evidence for shrub expansion in Northern Alaska  
825 and the Pan-Arctic, *Global change biology*, 12, 686-702, 10.1111/j.1365-2486.2006.01128.x,  
826 2006.

827 Tarnocai, C., Canadell, J. G., Schuur, E. A. G., Kuhry, P., Mazhitova, G., and Zimov, S.: Soil  
828 organic carbon pools in the northern circumpolar permafrost region, *Global Biogeochemical  
829 Cycles*, 23, n/a-n/a, 10.1029/2008gb003327, 2009.

830 Thullner, M., Van Cappellen, P., and Regnier, P.: Modeling the impact of microbial activity on  
831 redox dynamics in porous media, *Geochimica et Cosmochimica Acta*, 69, 5005-5019,  
832 10.1016/j.gca.2005.04.026, 2005.

833 Todd-Brown, K. E. O., Hopkins, F. M., Kivlin, S. N., Talbot, J. M., and Allison, S. D.: A  
834 framework for representing microbial decomposition in coupled climate models,  
835 *Biogeochemistry*, 109, 19-33, 10.1007/s10533-011-9635-6, 2011.

836 Todd-Brown, K. E. O., Randerson, J. T., Post, W. M., Hoffman, F. M., Tarnocai, C., Schuur, E.  
837 A. G., and Allison, S. D.: Causes of variation in soil carbon simulations from CMIP5 Earth  
838 system models and comparison with observations, *Biogeosciences*, 10, 1717-1736, 10.5194/bg-  
839 10-1717-2013, 2013.

840 Treseder, K. K., Balsler, T. C., Bradford, M. A., Brodie, E. L., Dubinsky, E. A., Eviner, V. T.,  
841 Hofmockel, K. S., Lennon, J. T., Levine, U. Y., MacGregor, B. J., Pett-Ridge, J., and Waldrop,  
842 M. P.: Integrating microbial ecology into ecosystem models: challenges and priorities,  
843 *Biogeochemistry*, 109, 7-18, 10.1007/s10533-011-9636-5, 2011.

844 W. D. Billings, K. M. P., G. R. Shaver, A. W. Trent: Root Growth, Respiration, and Carbon  
845 Dioxide Evolution in an Arctic Tundra Soil, *Arctic and Alpine Research*, 9, 129-137,  
846 10.1080/00040851.1977.12003908, 1977.



847 [Wang, G., M. A. M., Lianhong Gu, Christopher W. Schadt: Representation of Dormant and](#)  
848 [Active Microbial Dynamics for Ecosystem Modeling, Public Library of Science, 9,](#)  
849 [10.1371/journal.pone.0089252.g001, 2014.](#)

850 Wang, G., Jagadamma, S., Mayes, M. A., Schadt, C. W., Steinweg, J. M., Gu, L., and Post, W.  
851 M.: Microbial dormancy improves development and experimental validation of ecosystem  
852 model, *The ISME journal*, 9, 226-237, 10.1038/ismej.2014.120, 2015.

853 Wang Wei, F. J., T. Oikawa: Contribution of Root and Microbial Respiration to Soil CO<sub>2</sub> Efflux  
854 and Their Environmental Controls in a Humid Temperate Grassland of Japan, *Pedosphere*, 19,  
855 31-39, 2009.

856 Werf, H. V. d., and Verstraete, W.: Estimation of active soil microbial biomass by mathematical  
857 analysis of respiration curves: relation to conventional estimation of total biomass, *Soil Biology*  
858 *and Biochemistry*, 19, 267-271, 1987.

859 White, A., Cannell, M. G. R., and Friend, A. D.: The high-latitude terrestrial carbon sink: a  
860 model analysis *Global change biology*, 6, 227-245, 2000.

861 Wieder, W. R., Bonan, G. B., and Allison, S. D.: Global soil carbon projections are improved by  
862 modelling microbial processes, *Nature Climate Change*, 3, 909-912, 10.1038/nclimate1951,  
863 2013.

864 Xu, X., Schimel, J. P., Thornton, P. E., Song, X., Yuan, F., and Goswami, S.: Substrate and  
865 environmental controls on microbial assimilation of soil organic carbon: a framework for Earth  
866 system models, *Ecology letters*, 17, 547-555, 10.1111/ele.12254, 2014.

867 Zha, J., and Zhuang, Q.: Microbial decomposition processes and vulnerable arctic soil organic  
868 carbon in the 21st century, *Biogeosciences*, 15, 5621-5634, 10.5194/bg-15-5621-2018, 2018a.

869 Zha, J., and Zhuang, Q.: Microbial decomposition processes and vulnerable Arctic soil organic  
870 carbon in the 21st century, *Biogeosciences Discussions*, 1-34, 10.5194/bg-2018-241, 2018b.

871 Zhou, L., Tucker, C. J., Kaufmann, R. K., Slayback, D., Shabanov, N. V., and Myneni, R. B.:  
872 Variations in northern vegetation activity inferred from satellite data of vegetation index during  
873 1981 to 1999, *Journal of Geophysical Research: Atmospheres*, 106, 20069-20083,  
874 10.1029/2000jd000115, 2001.

875 Zhuang, Q., Romanovsky, V. E., and McGuire, A. D.: Incorporation of a permafrost model into a  
876 large-scale ecosystem model: Evaluation of temporal and spatial scaling issues in simulating soil  
877 thermal dynamics, *Journal of Geophysical Research: Atmospheres*, 106, 33649-33670,  
878 10.1029/2001jd900151, 2001.

879 Zhuang, Q., McGuire, A. D., O'Neill, K. P., Harden, J. W., Romanovsky, V. E., and Yarie, J.:  
880 Modeling soil thermal and carbon dynamics of a fire chronosequence in interior Alaska, *Journal*  
881 *of Geophysical Research*, 108, 10.1029/2001jd001244, 2002.

882 Zhuang, Q., He, J., Lu, Y., Ji, L., Xiao, J., and Luo, T.: Carbon dynamics of terrestrial  
883 ecosystems on the Tibetan Plateau during the 20th century: an analysis with a process-based  
884 biogeochemical model, *Global Ecology and Biogeography*, 19, 649-662, 10.1111/j.1466-  
885 8238.2010.00559.x, 2010.

886 Zhuang, Q., Zhu, X., He, Y., Prigent, C., Melillo, J. M., David McGuire, A., Prinn, R. G., and  
887 Kicklighter, D. W.: Influence of changes in wetland inundation extent on net fluxes of carbon  
888 dioxide and methane in northern high latitudes from 1993 to 2004, *Environmental Research*  
889 *Letters*, 10, 095009, 10.1088/1748-9326/10/9/095009, 2015.

890 Zhuang, Q., McGuire, A. D., Melillo, J. M., Klein, J. S., Dargaville, R. J., Kicklighter, D. W.,  
891 Myneni, R. B., Dong, J., Romanovsky, V. E., Harden, J., and Hobbie, J. E.: Carbon cycling in  
892 extratropical terrestrial ecosystems of the Northern Hemisphere during the 20th century: a



893 modeling analysis of the influences of soil thermal dynamics, *Tellus B: Chemical and Physical*  
894 *Meteorology*, 55, 751-776, 10.3402/tellusb.v55i3.16368, 2016.

895  
896  
897  
898

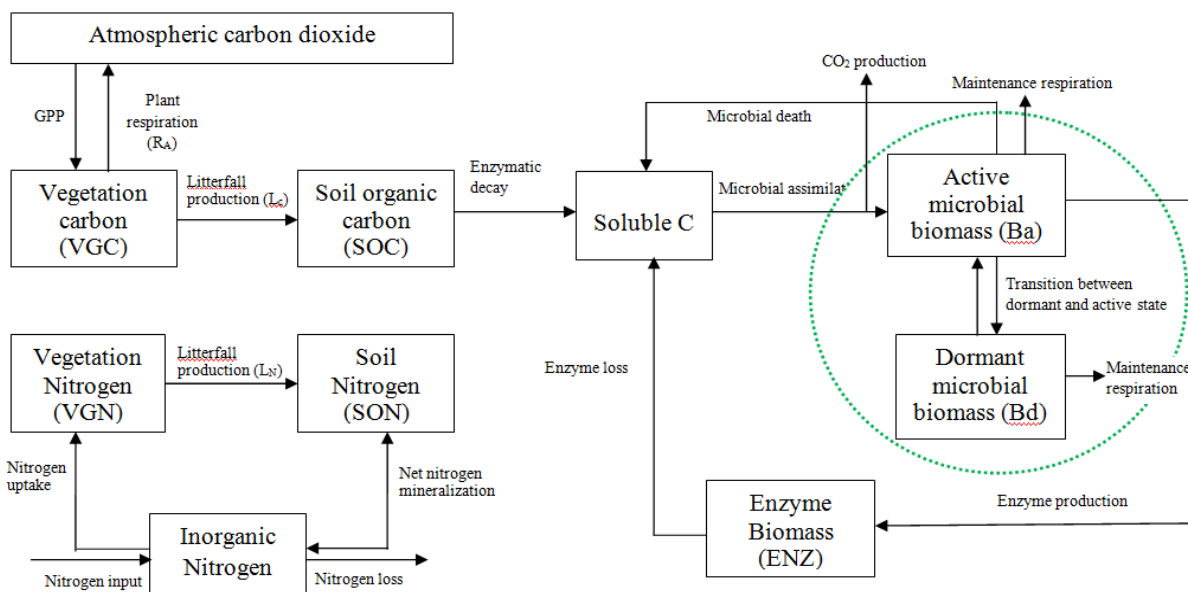
899 **Author contributions.** Q.Z. designed the study. J.Z. conducted model development, simulation  
900 and analysis. J.Z. and Q. Z. wrote the paper.

901 **Competing financial interests.** The submission has no competing financial interests.

902 **Materials & Correspondence.** Correspondence and material requests should be addressed to  
903 qzhuang@purdue.edu.

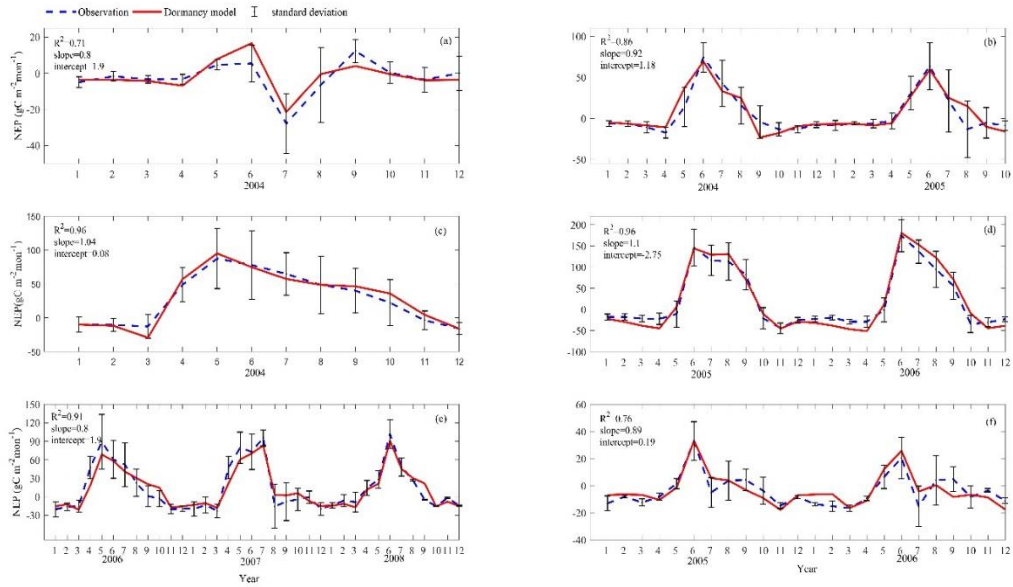
904

905



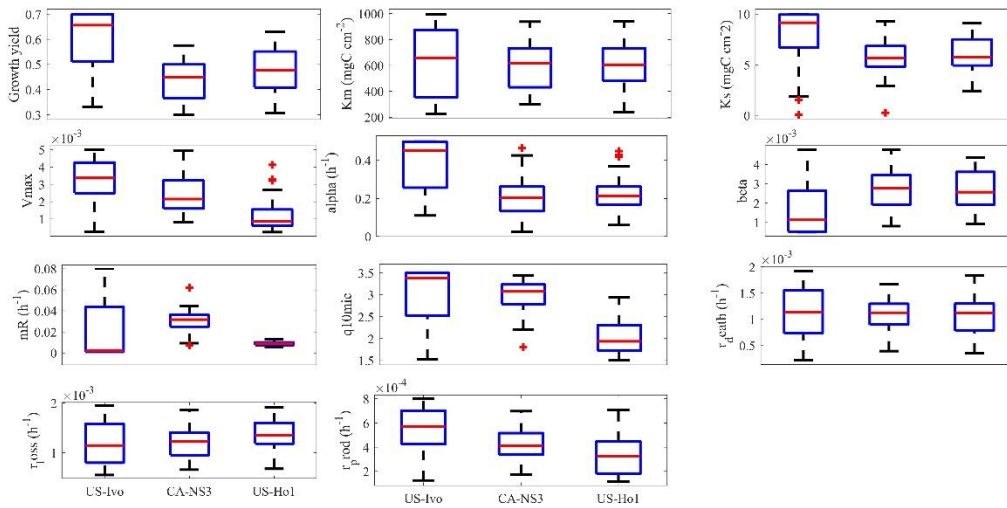
906  
907 **Figure 1.** Framework of the dormancy model: microbial biomass is split into two parts, active  
908 microbial biomass and dormant microbial biomass (shown in the green dashed circle).  
909 Maintenance respiration from these two parts, and the  $CO_2$  production through microbial  
910 assimilation contributes to heterotrophic respiration. The model was revised based on Zha &  
911 Zhuang (2018).

912

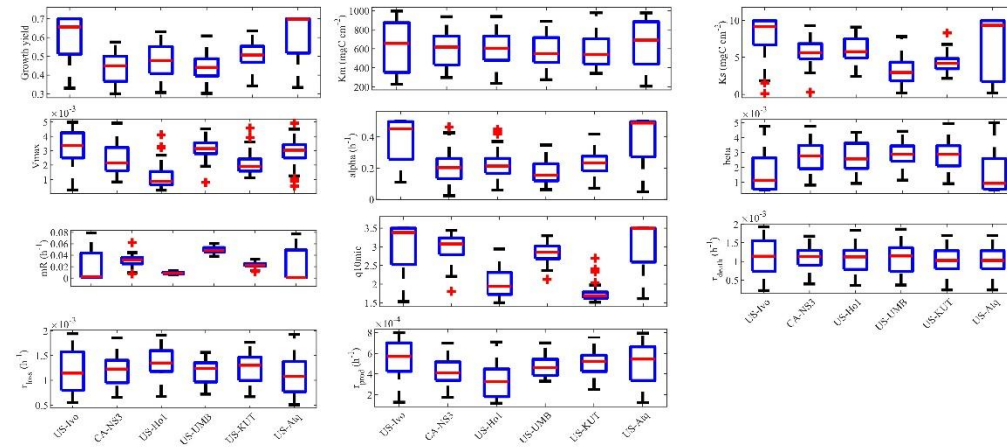


913  
 914 Figure 2. Comparison between observed and simulated NEP ( $\text{gC m}^{-2}\text{mon}^{-1}$ ) at: (a) Ivotuk (alpine  
 915 tundra), (b) UCI-1964 burn site (boreal forest), (c) Howland Forest (main tower) (temperate  
 916 coniferous forest), (d) Univ. of Mich. Biological Station (Temperate deciduous forest), (e)  
 917 KUOM Turfgrass Field (Grassland), and (f) Atqasuk (Wet tundra). Note: scales are different.  
 918 Error bars represent standard errors among daily measure data in one month.  
 919

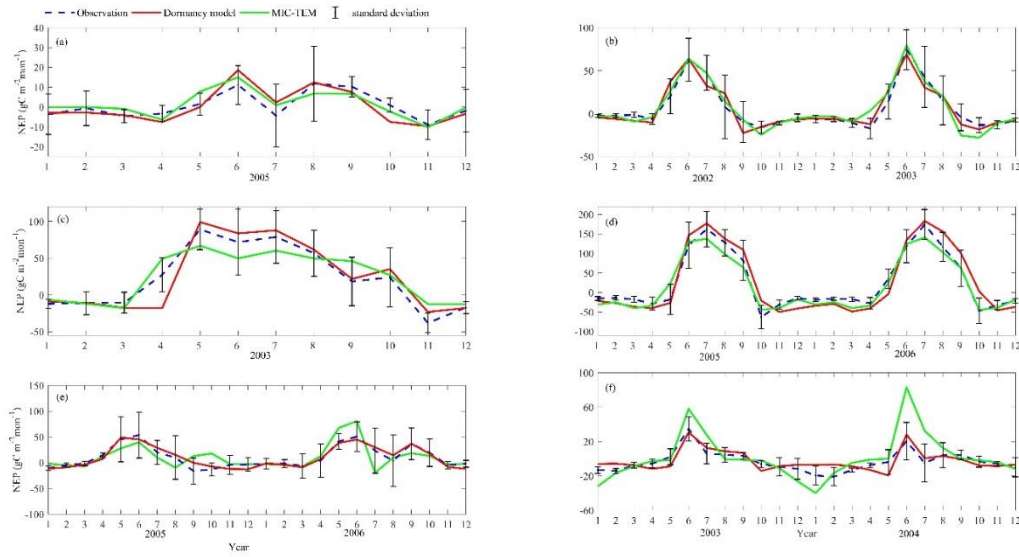
920



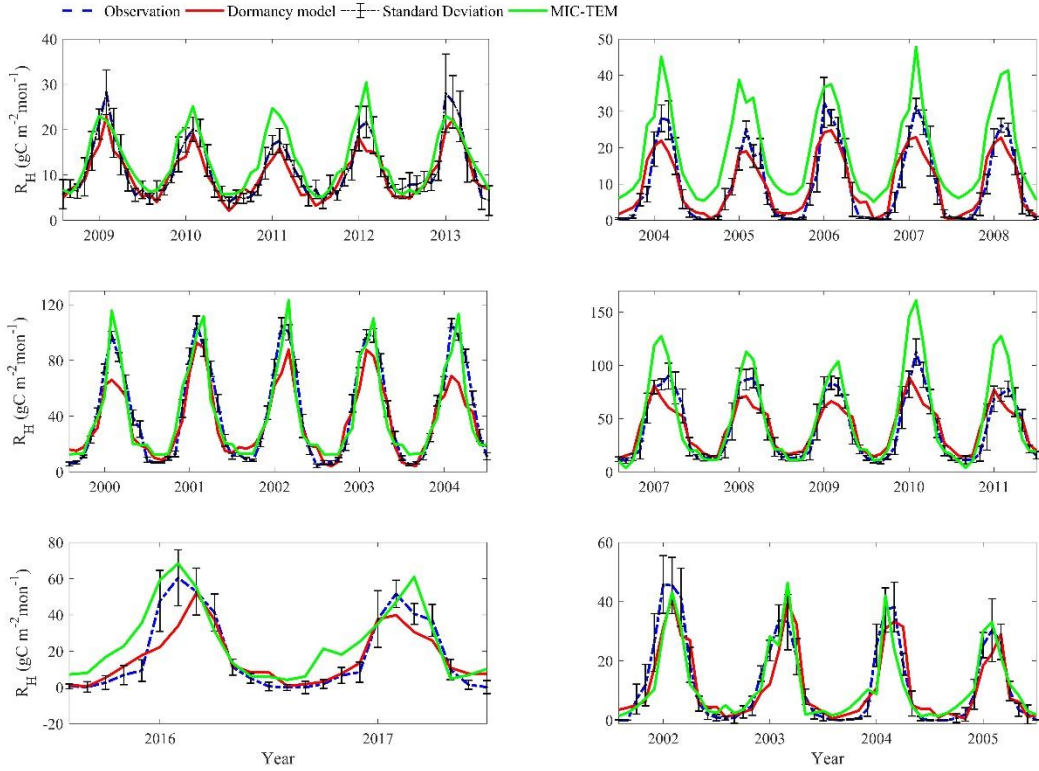
921



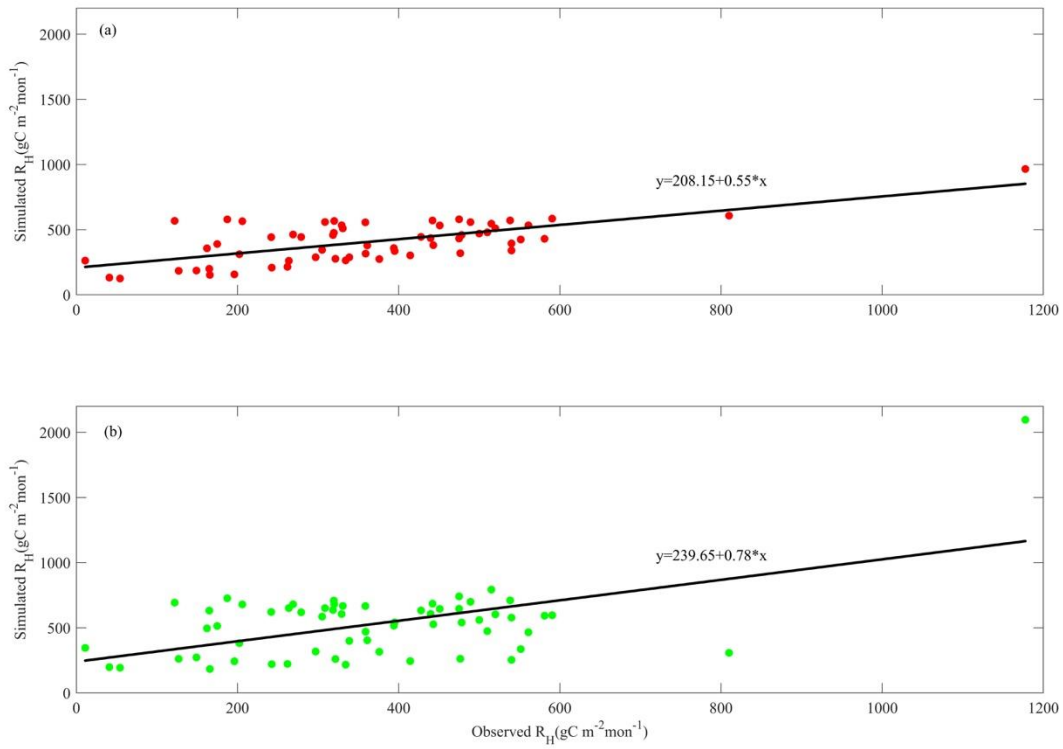
922 Figure 3. Boxplot of parameter posterior distribution that are obtained after ensemble inverse  
 923 modeling for MIC-TEM-dormancy all six sites: US-Ivo: Ivotuk (alpine tundra), CA-NS3: UCI-  
 924 1964 burn site (boreal forest), US-Ho1: Howland Forest (temperate coniferous forest), US-UMB:  
 925 Univ. of Mich. Biological Station (temperate deciduous forest), US-KUT: KUOM Turfgrass  
 926 Field (grassland), US-Atq: Atqasuk (wet tundra).  
 927



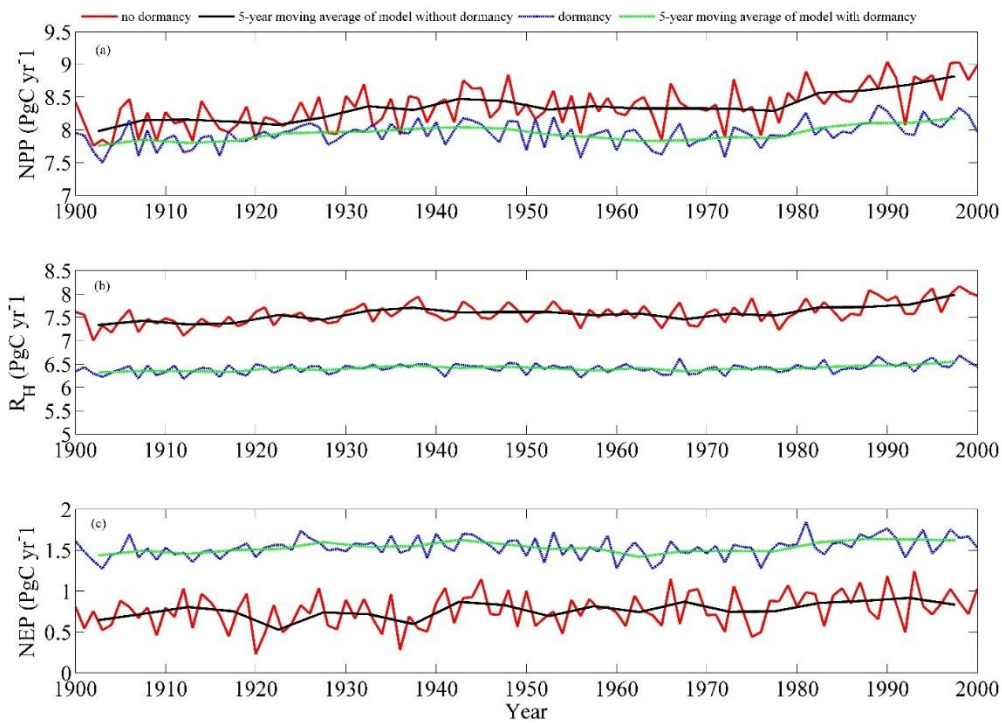
928  
 929 Figure 4. Comparison between observed and simulated NEP ( $\text{gC m}^{-2}\text{mon}^{-1}$ ) at: (a) Igotuk (alpine  
 930 tundra), (b) UCI-1964 burn site (boreal forest), (c) Howland Forest (main tower) (temperate  
 931 coniferous forest), (d) Bartlett Experimental Forest (Temperate deciduous forest), (e) Brookings  
 932 (Grassland), and (f) Atqasuk (Wet tundra). Note: scales are different.  
 933



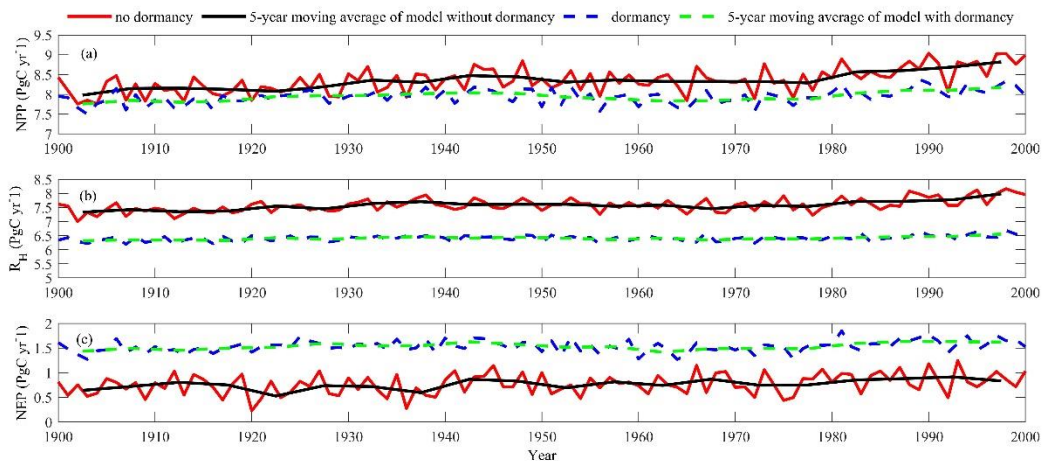
934  
 935 Figure 5. Comparison between observed and simulated  $R_H$  ( $\text{gC m}^{-2} \text{mon}^{-1}$ ) at: (a) US-EML (alpine  
 936 tundra), (b) CA-SJ2 (boreal forest), (c) US-Ho2 (temperate coniferous forest), (d) US-UMB  
 937 (Temperate deciduous forest), (e) US-Ro4 (Grassland), and (f) RU-Che (Wet tundra). Note:  
 938 scales are different.



939  
 940 Figure 6. Linear regression between simulated and observed annual  $R_H$  ( $\text{gC m}^{-2} \text{yr}^{-1}$ ) for: (a) MIC-  
 941 TEM-dormancy, and (b) MIC-TEM.  
 942

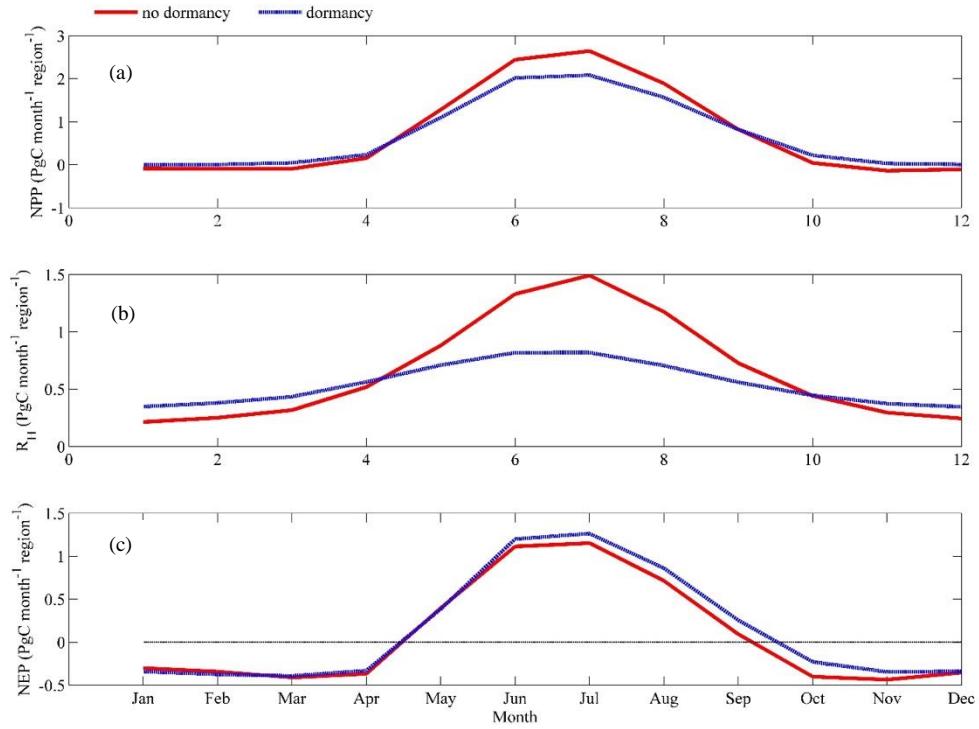


943



944

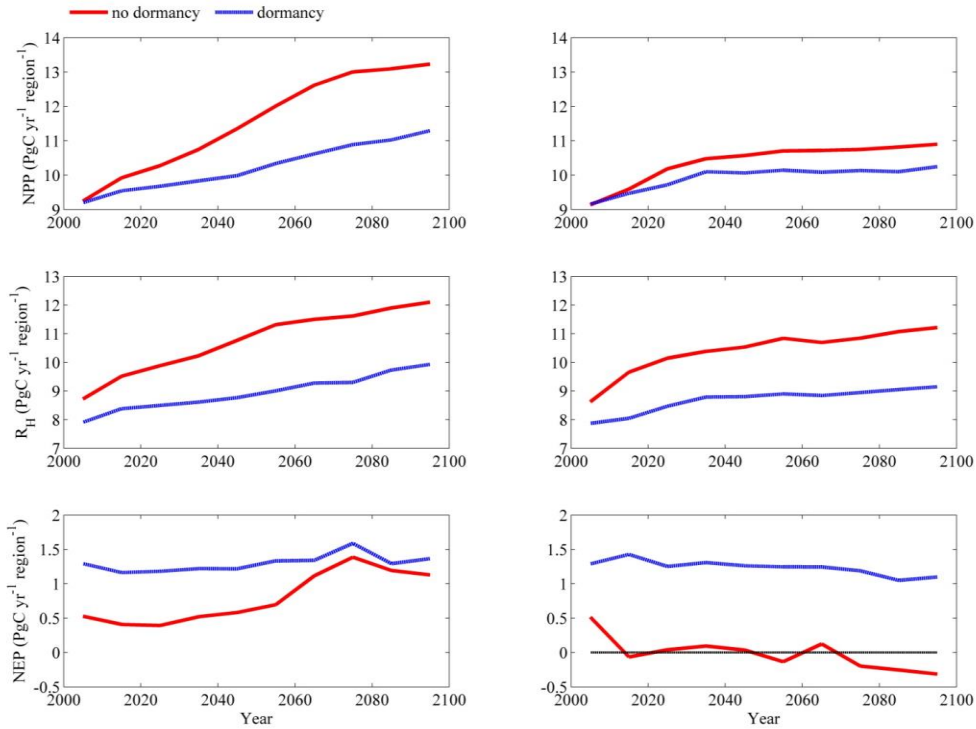
945 Figure 7. Simulated annual net primary production (NPP, top panel), heterotrophic respiration ( $R_H$ ,  
 946 center panel) and net ecosystem production (NEP, bottom panel) during the 20<sup>th</sup> century by  
 947 dormancy model and MIC-TEM, respectively.



948

949 Figure 8. Annual seasonal pattern of simulated (a) net primary production (NPP, top panel), (b)  
 950 heterotrophic respiration ( $R_H$ , center panel) and (c) net ecosystem production (NEP, bottom  
 951 panel) during the 1990s from dormancy model and MIC-TEM.





952

953 Figure 9. Predicted changes in carbon fluxes: (i) NPP, (ii)  $R_H$ , and (iii) NEP for all land areas north  
 954 of  $45^\circ\text{N}$  in response to transient climate change under the RCP 8.5 scenario (left panel) and RCP  
 955 2.6 scenario (right panel) with dormancy model and MIC-TEM, respectively. The decadal running  
 956 mean is applied.

957

958

959

960

961

962

963

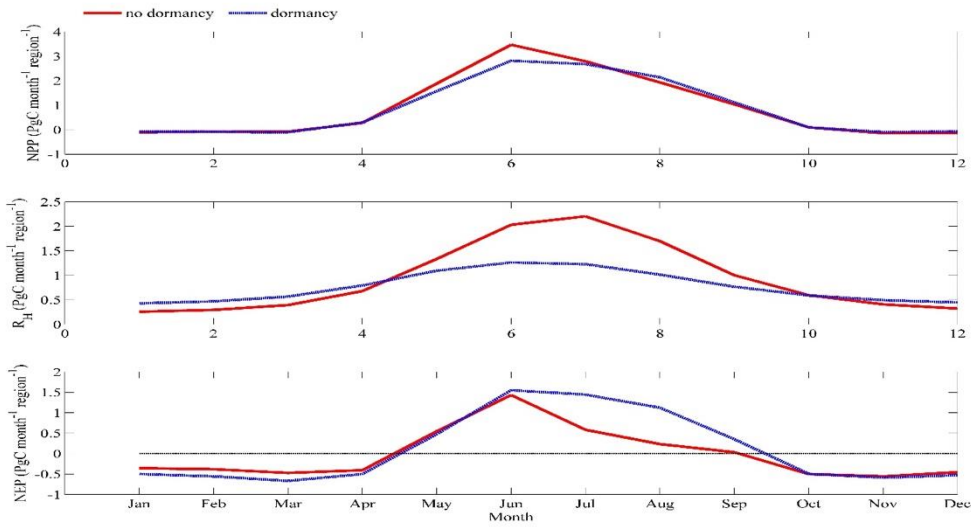
964

965

966

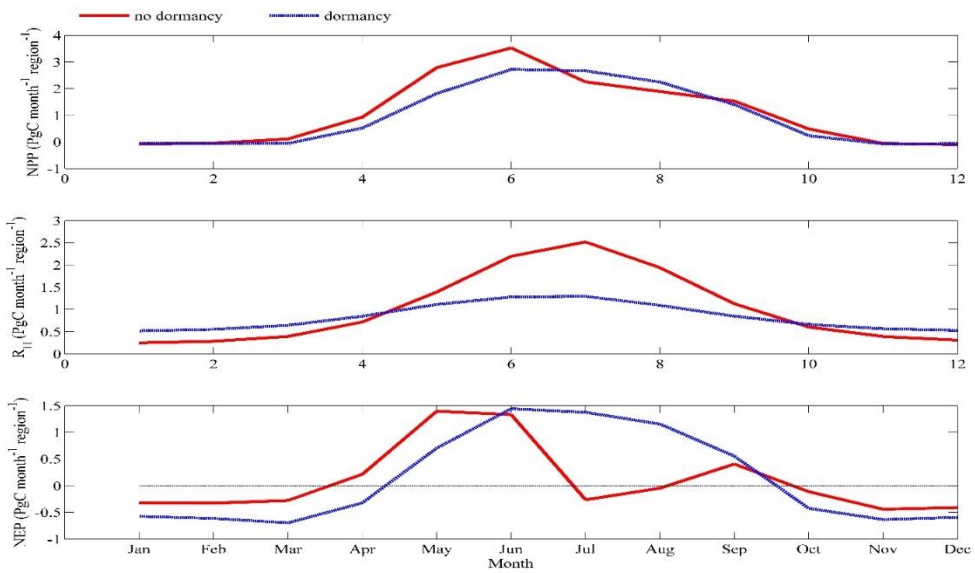
967

968 (a)



969

970 (b)



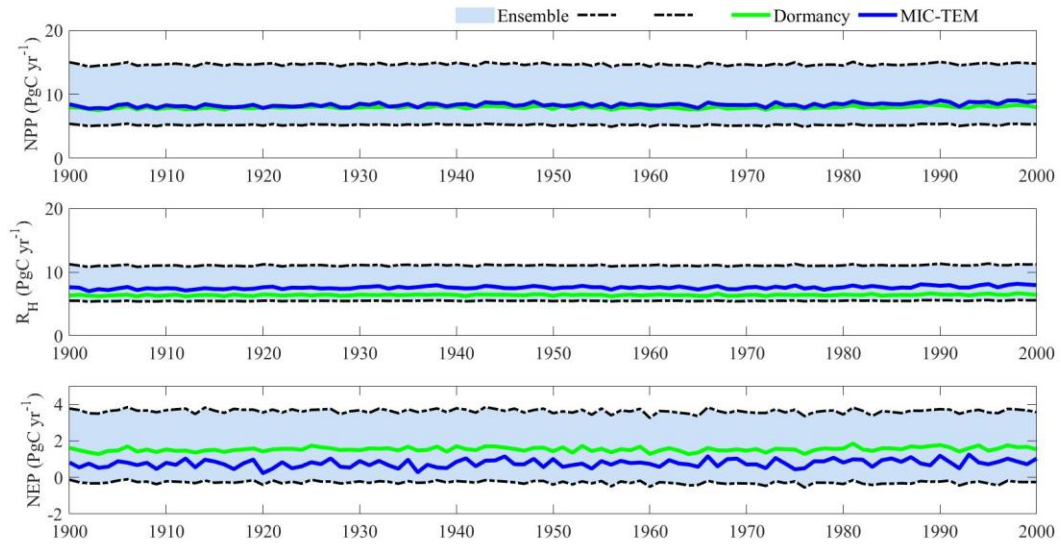
971

972 Figure 10. Annual seasonal pattern of simulated net primary production (NPP, top panel),  
973 heterotrophic respiration (R<sub>H</sub>, center panel) and net ecosystem production (NEP, bottom panel)  
974 during the 2090s from dormancy model and MIC-TEM under: (a) RCP 2.6 scenario (top panel)  
975 and (b) RCP 8.5 scenario (bottom panel).

976

977

978

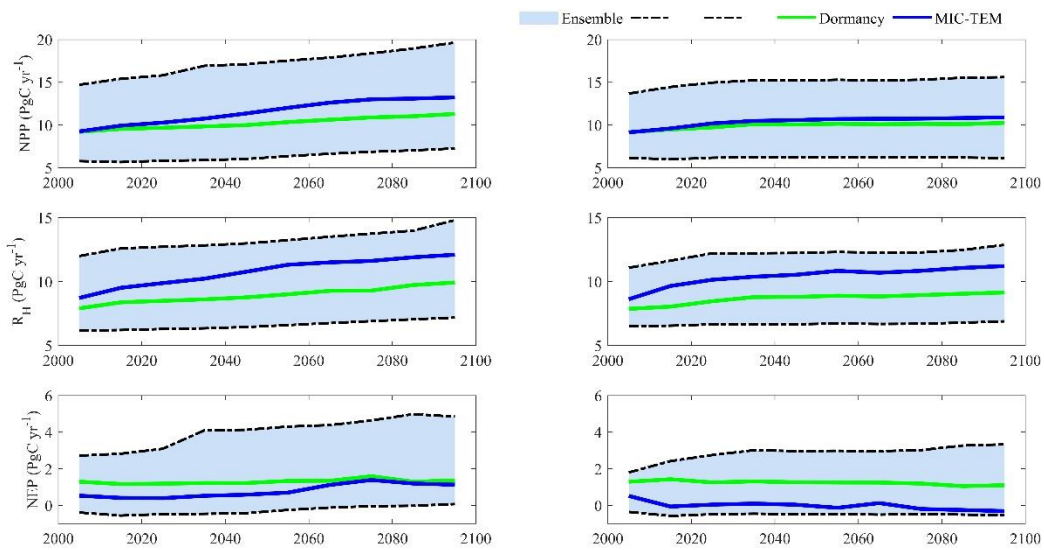


979  
 980  
 981  
 982  
 983  
 984  
 985  
 986  
 987  
 988  
 989  
 990  
 991  
 992  
 993  
 994  
 995  
 996  
 997  
 998  
 999  
 1000  
 1001  
 1002  
 1003  
 1004  
 1005  
 1006  
 1007  
 1008  
 1009

---

Figure 11. Simulated annual net primary production (NPP, top panel), heterotrophic respiration ( $R_H$ , center panel) and net ecosystem production (NEP, bottom panel) by MIC-TEM-dormancy with ensemble of parameters.

1010  
1011  
1012



1013  
1014  
1015  
1016  
1017  
1018  
1019

Figure 12. Simulated annual net primary production (NPP, top panel), heterotrophic respiration ( $R_H$ , center panel) and net ecosystem production (NEP, bottom panel) under RCP 8.5 scenario (left panel) and RCP 2.6 scenario (right panel) by MIC-TEM-dormancy with ensemble of parameters. The decadal running mean is applied. The grey area represents the upper and lower bounds of simulations.

1020 **Table 1. Parameters associated with detailed microbial dormancy in MIC-TEM-dormancy**  
 1021

parameter	unit	description	Parameter range	references
$m_R$	$h^{-1}$	Specific maintenance rate at active state	[0.001, 0.08]	Wang et al. (2014)
$Q_{10mic}$	-	Temperature effects on microbial metabolic activity (rate change per 10 °C increase in temperature). Based on 0.65 eV activation energy for soils	[1.5, 3.5]	He et al. (2015)
$Q_{10enz}$	-	Temperature effects on enzyme activity (rate change per 10 °C increase in temperature). Based on 6% rate increase per degree Celsius	1.79	He et al. (2015)
$\alpha$	-	the ratio of $m_R$ to the sum of maximum specific growth rate	[0.01, 0.5]	Wang et al. (2014)
$\beta$	-	Ratio of dormant microbial maintenance rate to $m_R$	[0.0005, 0.005]	Wang et al. (2014)
$Y_g$	-	carbon use efficiency	[0.3, 0.7]	He et al. (2015)
$K_s$	$mgC\ cm^{-2}$	Half-saturation constant for directly accessible substrate	[0.01, 10]	Wang et al. (2014)
$K_{muptake}$	$mgC\ cm^{-2}$	Half-saturation constant for enzymatic decay of SOC	[200, 1000]	He et al. (2015)
$r_{death}$	$h^{-1}$	Potential rate of microbial death	$[2e^{-4}, 2e^{-3}]$	Allison et al. (2010)
$r_{EnzProd}$	$h^{-1}$	Enzyme production rate of microbe	$[1e^{-4}, 8e^{-4}]$	He et al. (2015)
$r_{enzloss}$	$h^{-1}$	Enzyme loss rate	[0.0005, 0.002]	Allison et al. (2010)
$V_{max}$	$mgC\ cm^{-2}\ h^{-1}$	Maximum SOC decay rate	$[1e^{-4}, 5e^{-3}]$	He et al. (2015)

1022  
 1023  
 1024

1025 **Table 2. Site description and measured NEP data used to calibrate MIC-TEM-dormancy**

Site Name	Location (Longitude (degrees) /Latitude (degrees))	Elevation (m)	Vegetation type	Description	Data range	Citations
Univ. of Mich. Biological Station	84.71W 45.56 N	234	Temperate deciduous forest	Located within a protected forest owned by the University of Michigan. Mean annual temperature is 5.83° C with mean annual precipitation of 803mm	01/2005- 12/2006	Gough et al. (2013)
Howland Forest (main tower)	68.74W 45.20N	60	Temperate coniferous forest	Closed coniferous forest, minimal disturbance.	01/2004- 12/2004	Davidson et al. (2006)
UCI-1964 burn site	98.38W 55.91N	260	Boreal forest	Located in a continental boreal forest, dominated by black spruce trees, within the BOREAS northern study area in central Manitoba, Canada.	01/2004- 10/2005	Goulden et al. (2006)
KUOM Turfgrass Field	93.19W 45.0N	301	Grassland	A low-maintenance lawn consisting of cool-season turfgrasses.	01/2006- 12/2008	Hiller et al. (2011)
Atqasuk	157.41W 70.47N	15	Wet tundra	100 km south of Barrow, Alaska. Variety of moist-wet coastal sedge tundra, and moist-tussock tundra surfaces in the more well-drained upland.	01/2005- 12/2006	Oechel et al. (2014);
Ivotuk	155.75W 68.49N	568	Alpine tundra	300 km south of Barrow and is located at the foothill of the Brooks Range and is classified as tussock sedge, dwarf-shrub, moss tundra.	01/2004- 12/2004	McEwing et al. (2015)

1026  
1027  
1028  
1029

1030 **Table 3. Site description and measured NEP data used to validate MIC-TEM-dormancy**

1031

Site Name	Location (Longitude (degrees) /Latitude (degrees))	Elevation (m)	Vegetation type	Description	Data range	Citations
Bartlett Experimental Forest	71.29W/ 44.06N	272	Temperate deciduous forest	Located within the White Mountains National Forest in north-central New Hampshire, USA, with mean annual temperature of 5.61 °C and mean annual precipitation of 1246mm.	01/2005- 12/2006	Jenkins et al. (2007); Richardson et al. (2007);
Howland Forest (main tower)	68.74W/ 45.20N	60	Temperate coniferous forest	Closed coniferous forest, minimal disturbance.	01/2003- 12/2003	Davidson et al. (2006)
UCI-1964 burn site	98.38W/ 55.91N	260	Boreal forest	Located in a continental boreal forest, dominated by black spruce trees, within the BOREAS northern study area in central Manitoba, Canada.	01/2002- 12/2003	Goulden et al. (2006)
Brookings	96.84W/ 44.35N	510	Grassland	Located in a private pasture, belonging to the Northern Great Plains Rangelands, the grassland is representative of many in the north central United States, with seasonal winter conditions and a wet growing season.	01/2005- 12/2006	Gilmanov et al. (2005)
Atqasuk	157.41W/ 70.47N	15	Wet tundra	100 km south of Barrow, Alaska. Variety of moist-wet coastal sedge tundra, and moist-tussock tundra surfaces in the more well-drained upland.	01/2003- 12/2004	Oechel et al. (2014);
Ivotuk	155.75W/ 68.49N	568	Alpine tundra	300 km south of Barrow and is located at the foothill of the Brooks Range and is classified as tussock sedge, dwarf-shrub, moss tundra.	01/2005- 12/2005	McEwing et al. (2015)

1032

1033 **Table 4. Site description and measured  $R_H$  data used to validate MIC-TEM-dormancy model**

1034  
1035  
1036  
1037  
1038  
1039  
1040  
1041  
1042  
1043  
1044  
1045

Site	Location (Longitude (degrees) /Latitude (degrees))	Elevation (m)	Vegetation type	Data range	Citations
US-EML	149.25W/ 63.88N	700	Alpine tundra	01/2009- 12/2013	Belshe et al. (2012)
CA-SJ2	104.65W/ 53.95N	580	Boreal forest	01/2004- 12/2008	Coursolle et al. (2006)
US-Ho2	68.75W/ 45.21N	91	Temperate coniferous forest	01/2000- 12/2004	Davidson et al. (2006)
US-UMB	84.71W/ 45.56N	234	Temperate deciduous forest	01/2005- 12/2006	<b>Gough</b> et al. (2013)
US-Ro4	93.07W/ 44.68N	274	Grasslands	01/2016- 12/2017	Griffis et al. (2011)
RU-Che	161.34E/ 68.61N	6	Wet tundra	01/2002- 12/2005	Merbold et al. (2009)



1046 **Table 5. Model validation statistics for Dormancy model and MIC-TEM at six sites with NEP data**

1047

1048

1049

1050

1051

1052

1053

1054

1055

1056

1057

1058

1059

1060

1061

1062

Site Name	Vegetation type	Models	Intercept	Slope	R-square	Adjusted R-square	p-value
Ivotuk	Alpine tundra	MIC-TEM	0.85	0.83	0.70	0.67	<0.001
		Dormancy	-0.51	1.09	0.75	0.73	<0.001
UCI-1964 burn site	Boreal forest	MIC-TEM	0.18	1.03	0.912	0.9080	<0.001
		Dormancy	-0.21	0.96	0.90	0.894	<0.001
Howland Forest (main tower)	Temperate coniferous forest	MIC-TEM	7.29	0.72	0.85	0.83	<0.001
		Dormancy	0.27	1.05	0.89	0.88	<0.001
Bartlett Experimental Forest	Temperate deciduous forest	MIC-TEM	-6.05	0.91	0.944	0.941	<0.001
		Dormancy	-2.34	1.13	0.93	0.924	<0.001
Brookings	Grassland	MIC-TEM	3.05	0.71	0.84	0.83	<0.001
		Dormancy	0.17	0.95	0.90	0.898	<0.001
Atqasuk	Wet tundra	MIC-TEM	7.22	1.85	0.71	0.70	<0.001
		Dormancy	0.19	0.82	0.67	0.66	<0.001

1063 **Table 6. Model validation statistics for Dormancy model and MIC-TEM at six sites with R<sub>H</sub> data**  
 1064

Site ID	Vegetation type	Models	Intercept	Slope	R-square	Adjusted R-square	RMSE	p-value
US-EML	Alpine tundra	MIC-TEM	2.90	0.91	0.79	0.78	3.55	<0.001
		Dormancy	1.81	0.74	0.87	0.85	2.69	<0.001
CA-SJ2	Boreal forest	MIC-TEM	7.59	1.12	0.84	0.83	9.8	<0.001
		Dormancy	2.6	0.74	0.86	0.85	3.97	<0.001
US-Ho2	Temperate coniferous forest	MIC-TEM	4.07	0.89	0.86	0.84	12.39	<0.001
		Dormancy	6.59	0.71	0.91	0.89	11.83	<0.001
US-UMB	Temperate deciduous forest	MIC-TEM	-4.73	1.32	0.81	0.8	20.05	<0.001
		Dormancy	13.6	0.67	0.85	0.84	12.94	<0.001
US-Ro4	Grassland	MIC-TEM	9.34	0.87	0.81	0.79	11.25	<0.001
		Dormancy	4.81	0.65	0.86	0.84	9.21	<0.001
RU-Che	Wet tundra	MIC-TEM	2.5	0.67	0.72	0.71	6.24	<0.001
		Dormancy	1.96	0.77	0.81	0.79	5.95	<0.001